Non-linear and Non-stationary Influences of Geomagnetic Activity on the Winter North Atlantic Oscillation

Yun Li[a,1], Hua Lu[b], Martin J. Jarvis[b], Mark A. Clilverd[b], Bryson Bates[c]

Prepared for *Journal of Geophysical Research-Atmospheres*

11 May 2011

[1]Corresponding author Email: Yun.Li@csiro.au

[a] CSIRO Climate Adaptation Flagship, CSIRO Mathematics, Informatics and Statistics, Wembley, WA 6913, Australia.

[b] British Antarctic Survey, High Cross, Madingley Road, Cambridge CB3 0ET, England, U.K. (email: hlu@bas.ac.uk; mjja@bas.ac.uk ; macl@bas.ac.uk)

[c] CSIRO Climate Adaptation Flagship, CSIRO Marine & Atmospheric Research, Wembley, WA 6913, Australia. (email: Bryson.Bates@csiro.au)

Abstract: The relationship between the geomagnetic aa index and the winter North Atlantic Oscillation (NAO) has previously been found to be non-stationary, being weakly negative during the early 20th century and significantly positive since the1970s. The study reported here applies a statistical method called the Generalised Additive Modelling (GAM) to elucidate the underlying physical reasons.

We find that the relationship between *aa* index and the NAO during the Northern Hemispheric winter is generally non-linear and can be described by a concave shape with a negative relation for small to medium *aa* and a positive relation for medium to large *aa*. The non-stationary character of the *aa*-NAO relationship may be ascribed to two factors. Firstly, it is modulated by the multi-decadal variation of solar activity. This solar modulation is indicated by significant change points of the trends of solar indices around the beginning of solar cycle 14, 20 and 22 (*i.e.* ~1902/1903, ~1962/1963, and ~1995/1996). Coherent changes of the trend in the winter time NAO followed the solar trend changes a few years later. Secondly, the *aa*-NAO relationship is dominated by the *aa* data from the declining phase of even-numbered solar cycles, implying that the 27-day recurrent solar wind streams may be responsible for the observed *aa*-NAO relationship. It is possible that an increase of long-duration recurrent solar wind streams from high latitude coronal holes during solar cycles 20 and 22 may partially account for the significant positive *aa*-NAO relationship during the last 30 years of the 20th century.

47

48 1. Introduction

49 The North Atlantic Oscillation (NAO) is a dominant mode of broad-scale climate
50 variability in the Northern Hemisphere (NH) [*Hurrell*, 1995; *Hurrell et al.*, 2003]. Being
51 most active during winter months, it is directly linked to the variation of westerly winds,
52 orchestrates the strength and orientation of storm tracks, and dictates precipitation levels and
53 fluctuations in marine ecosystems over the Atlantic as well as the adjacent regions
54 [*Stephenson et al.*, 2000]. Positive NAO is associated with a net displacement of air from the
55 Arctic and Icelandic regions towards the subtropic belt near the Azores and the Iberian
56 Peninsula by strengthening westerly winds over the North Atlantic Ocean. Stronger
57 westerlies bring more warm moist air to the European continent and gives rise to milder
58 maritime winters. Negative NAO is associated with an opposite redistribution of air mass
59 between the Arctic and the subtropical Atlantic with weaker westerlies over the North
60 Atlantic. It corresponds to colder than normal European winters. It is critical to understand
61 the mechanisms that control and affect the NAO and its temporal evolution as it is associated
62 with large variations in weather and climate over much of the globe on interannual and longer
63 time scales [*Hurrell and Deser*, 2010].

64 Despite its importance, the fundamental mechanisms behind the variability of the NAO
65 remain in debate [*Hurrell and Deser*, 2010; *Saenger et al.*, 2009]. It has been suggested that
66 external forces might nudge the NAO to remain in either its positive or negative phase over
67 an extended period. Observations have shown that the NAO may be modulated by a multi-
68 decadal oscillation in Atlantic sea surface temperature [*Enfield et al.*, 2001; *Gray et al.*, 2004;
69 *Knight et al.*, 2006]. Low frequency variations of the NAO were previously attributed to
70 perturbations associated with the thermal storage effect of the ocean, sea-ice or snow [*Gong*

71 *et al.*, 2003; *Hall and Visbeck*, 2002; *Mehta et al.*, 2000; *Rodwell et al.*, 1999], or to
72 anthropogenic forcing and/or ozone depletion in the stratosphere [*Corti et al.*, 1999; *Gillett et*
73 *al.*, 2003; *Shindell et al.*, 1999; *Woollings et al.*, 2010a]. Studies based on those proposed
74 mechanisms have been carried out using general circulation models (GCMs) [*Gong et al.*,
75 2002; *Hoerling et al.*, 2001]. However, the simulated NAOs often exhibit little multi-decadal
76 variation compared with observations [*Osborn*, 2004]. In particular, it remains unclear what
77 has caused the enhanced inter-annual variability of the NAO over the last half of the 20th
78 century and a more positive trend of the NAO in 1970s to 1990s [*Feldstein*, 2002; *Hurrell*
79 *and Deser*, 2010].

80 It has also been suggested that changes in solar and geomagnetic activity may modulate
81 the NAO [*Bochnicek and Hejda*, 2005; *Kodera*, 2002; 2003]. *Kodera* [2002] and *Ogi et al*.
82 [2003] found that in winter the spatial and temporal structure of the NAO is greatly modified
83 by the 11-year solar cycle (11-yr SC). Stronger and more significant correlations were found
84 to exist between geomagnetic activity and the NAO than with the 11-yr SC [*Bochnicek and*
85 *Hejda*, 2005; *Thejll et al.*, 2003]. *Boberg and Lundstedt* [2002; 2003] found that the variation
86 of the winter NAO is correlated with the electric field strength of the solar wind, and
87 suggested a solar wind generated electromagnetic disturbance in the ionosphere may
88 dynamically propagate downward to the stratosphere and influence surface NAO. Changes of
89 temperature near the Atlantic basin have also been statistically linked to geomagnetic
90 perturbations [*Seppälä et al.*, 2009]. *Woollings et al*. [2010b] showed that a stronger signal in
91 the eastern part of the North Atlantic was associated with solar wind driven open solar flux
92 when compared with that associated with the F10.7-cm solar flux. *Lu et al*. [2008b] have
93 shown that there is a robust relationship between solar wind dynamic pressure and the
94 Northern Annular Mode (NAM), which resembles the behaviour of the NAO near the
95 surface. They showed that stratospheric wind and temperature variations are positively

96 projected onto the NAM when the 11-yr SC is at its maximum phase during winter, and
97 negatively projected onto the NAM during the 11-yr SC minimum phase in spring. *Paluš and*
98 *Novotná* [2007] found that there were common oscillatory modes in the geomagnetic *aa*-
99 index, the NAO and surface temperature. It has been also suggested that solar wind induced
100 geomagnetic activity may alter stratospheric chemistry through particle precipitation and
101 descent of odd Nitrogen (NOx) [*Randall et al.*, 2006; *Randall et al.*, 2007; 2005; *Solomon et*
102 *al.*, 1982]. Other studies suggested that solar wind induced geomagnetic activity may perturb
103 atmospheric circulation dynamically through a change in planetary wave reflection conditions
104 [*Arnold and Robinson*, 2001; *Lu et al.*, 2008a].

105 It has also been shown that solar activity may indirectly alter cloud cover *via* a
106 modulation of the galactic cosmic ray (GCR) flux [e.g. *Pudovkin and Veretenenko*, 1995;
107 1996; *Svensmark and Friis- Christensen*, 1997; *Svensmark et al*. 2009; *Harrison and*
108 *Stephenson*, 2006], while others found the GCR-cloud connection is rather weak [*Laken et*
109 *al*., 2009; *Pierce and Adams*, 2009]. Changes in solar wind electric fields may also perturb
110 the global electrical circuit, which extends into the lower atmosphere at high magnetic
111 latitudes, and consequently precipitation and cloud cover in the fair-weather part of the global
112 circuit [*Tinsley et al*., 2007; *Kniveton et al*., 2008]. Since the solar wind driven geomagnetic
113 activity also modulates the cosmic ray flux, it has been suggested that it may affect the
114 amount of tropospheric ionization and cloud cover [*Shaviv*, 2005].

115 While those statistical correlations suggest there might be a causal link between solar
116 wind driven geomagnetic activity and the NAO, a sound mechanism is required for better
117 understanding and to rule out coincidental correlations. What is most puzzling is that the
118 relationship between geomagnetic activity and the NAO appears to be non-stationary, being
119 significantly positive since the1970s and weakly negative in the early part of the 20th century

120 [*Bucha and Bucha*, 1998; *Palamara and Bryant*, 2004]. *Paluš and Novotná* [2009] found that
121 the phase coherence between the geomagnetic *aa* index and the NAO was statistically
122 significant only from the 1950's onwards while no significant phase coherence was found in
123 the earlier period. The non-stationary behavior of the *aa*-NAO relationship was attributed to
124 the much lower geomagnetic activity occurring in the early part of the 20th century than in
125 1950–2000 which led to a significant shift of atmospheric circulation patterns [*Bucha and*
126 *Bucha*, 1998]. It has also been suggested that the non-stationary behavior of the *aa*-NAO
127 relationship might be due to a multi-decadal scale modulation of the geomagnetic-NAO
128 relationship [*Thejll et al.*, 2003].

129 Geomagnetic activity is primarily driven by the solar wind which encounters the Earth's
130 magnetic field at the magnetopause. Solar wind is emitted from the Sun either as high-speed
131 wind streams from co-rotating interactive regions (CIRs) of coronal holes, transient wind
132 streams associated with coronal mass ejections (CMEs), or slow solar winds from the borders
133 of coronal holes [*Emery et al.*, 2009]. High-speed solar wind generated from CIRs tends to
134 recur with a ~27-day periodicity and is most prominent in the descending phases of SCs. It
135 has been noticed that the characteristics of the ~27-day periodicity in the geomagnetic *aa*
136 index are different during the decay phases of even- and odd-numbered SCs [*Cliver et al.*,
137 1996]. Studies have shown that recurrent activity was stronger following even-number
138 maxima [*Bumba and Hejna*, 1991; *Hapgood*, 1993; *Rangarajan*, 1991] and prominent 27-day
139 recurrent geomagnetic activity tends to persist longer during the decline of even-numbered
140 SCs than in odd-numbered ones [*Sargent*, 1985; 1986]. If, as postulated, geomagnetic activity
141 has an impact on the NAO and near surface climate, the 27-day recurrence events may have a
142 detectable effect on the interannual and longer-term variations of the NAO. Thus, a step
143 towards examining such a possibility would be to examine whether or not the *aa*-NAO
144 relationship becomes more distinct during the declining phase of even-numbered SCs.

In this study, we re-examine the *aa*-NAO relationship in order to elucidate the underlying physical reasons for its non-stationary behavior. Like previous studies, we focus on the most dynamically active season, *i.e*., the extended NH winter period from December to March for the period of 1868-2009. We first apply a statistical method called Generalised Additive Modelling (GAM) [*Wood*, 2006; 2008] to search for statistically significant linear and/or non-linear relationships between the *aa* index and the NAO for the period of 1868-2009. We then use the Sequential Mann-Kendall (SMK) test [*Gerstengarbe and Werner*, 1999] to study the multi-decadal variation of the NAO and its possible link to the change points in the trends of solar and geomagnetic indices. We investigate the non-stationary behavior of the *aa*-NAO relationship by building non-linear and linear regression models using the GAM technique for each sub-period separated by two nearby change point years that are identified by the SMK test. In order to examine whether or not the recurrent solar wind events play a role in determining the *aa*-NAO relationship, the linear models and GAMs are also built based on the data grouped according to the ascending/declining phases of odd/even number SCs.

2. Data

The NAO time series used here is the normalized difference between the sea level atmospheric pressures at Gibraltar and South-West Iceland. The monthly pressure at each location is normalised by subtracting the mean and dividing by the standard deviation. A standard period (1951–1980), instead of the whole recording period, is considered for estimating the mean and the standard deviation [*Jones et al.*, 1997]. Monthly NAO indices since 1821 have been downloaded from the website of Climate Research Unit of the University of East Anglia, UK (http://www.cru.uea.ac.uk). Due to the large amount of missing data before 1824, the time series of December to March mean (denoted as NAO_{DJFM} hereafter) used here only covers the period of 1825-2009. The year of NAO_{DJFM} is defined by

the year in January. That is: 1825 NAO_{DJFM} represents the mean NAO value for the 1824/1825 winter and so forth.

The geomagnetic *aa* index [*Mayaud*, 1972] is commonly used to monitor the reactions of Earth's upper atmosphere (*e.g*. magnetosphere and ionosphere) and magnetic field to changes in the incoming solar wind. The monthly *aa* index from 1st of January 1868 to 31st of December 2009 is used here. Its winter averages were calculated in the same way as that used for NAO_{DJFM} and are denoted as aa_{DJFM} hereafter.

Three different solar input data sets are used to study multi-decadal variation of solar activity and its possible modulation effect on the *aa*-NAO relationship. The first one is the sunspot number (R_z), a commonly used proxy for the phase of the given SC at century time scales. It is also a proxy for solar electromagnetic radiation which creates and maintains the earth's ionosphere and the tidal winds in the atmosphere. Monthly international sunspot number data from Jan. 1749 to Dec. 2009 are used here; they are available at http://www.ngdc.noaa.gov/ . The second and third solar data sets are solar sunspot area in the Sun's northern hemisphere (NSSA) and the solar North-South asymmetry index $As = (N–S)/(N+S)$ where N and S are the total sunspot area in the solar northern and southern hemispheres, respectively. The asymmetry index *As* is characterized by the time dependence of various activity indices in two hemispheres of the Sun which often display mismatch in both phase and power spectra [e.g. *Li et al*., 2002]. The reason we extend our analysis to include *As* here is because many studies have shown that it represents a fundamental characteristic of solar activity, which is controlled by solar magnetic fields instead of by the 11-yr solar cycle [*Badalyan and Obridko*, 2011 and references therein]. Monthly sunspot area and its north-south asymmetry are available at http://solarscience.msfc.nasa.gov/greenwch.shtml; this data set contains measurements collected by the Royal Greenwich Observatory (May, 1874 – Dec., 1975) and by the US Air

195 Force (1976 – present). The mismatch between the two different instruments pre-1975 and
196 after 1975 was calibrated by Dr. David Hathaway at NOAA/NASA by using the additional
197 data from the Mount Wilson photographic plate collection from 1917 to 1982. The December
198 to March mean *NSSA* and *As* from the period of 1874 to 2009 are used here.

199 **3. Methods**

200 For the first time, a non-parametric regression method called Generalized Additive
201 Model (GAM) [*e.g.*, *Gu*, 2002; *Hastie and Tibshirani*, 1990; *Wood*, 2006; 2008] is used to
202 build statistical relationships between the winter NAO and the geomagnetic *aa* index. GAM
203 is a statistical modeling framework which blends a generalized linear model (GLM) with
204 additive terms, in which some of the terms in the model are fitted as smooth, non-linear
205 functions of the explanatory variables. Rather than pre-specifying the form of the function,
206 the data are used to estimate the shape of smooth functions. This provides a more flexible
207 modeling approach (than GLM) which allows the users to explore the non-linear relationship
208 between the response and the explanatory variables. GAM has been used extensively in the
209 analysis of air pollution, health, environment and ecology [e.g.,*He et al.*, 2006; *Liu et al.*,
210 2009; *McLeod and Pople*, 2010; *Mikolajczyk et al.*, 2010] due to its flexibility to model the
211 relationship between the predicands and predictors. More recently, GAMs have been applied
212 to hydrological and climatic research areas [e.g., *Cox et al.*, 2005; *Mestre and Hallegatte*,
213 2009; *Morton and Henderson*, 2008]. A brief description of GAM is given in Appendix 1.

214 The sequential Mann-Kendall (SMK) test [*Gerstengarbe and Werner*, 1999] is employed
215 to detect the approximate times when a significant change of trend occurs in a given time
216 series. It is a non-parametric test and comes under the class of rank tests and has been
217 frequently used to detect approximate potential trend change points in a time series [*Seneyers*,
218 1990; *Taubenheim*, 1989]. For a given sampling series, the test is carried out by ranking the
219 progressive and retrograde score series of this sample. The null hypothesis is that there is no

turning point in the trend of the sampled time series under investigation. In order to prove or to disprove the null hypothesis, the statistical procedure introduced by *Gerstengarbe and Werner* [1999] is used. See Appendix 2 for mathematical details. As the method can only detect the *approximate* time when a change of the trend may occur, we find that it is often the case that multiple changes can be detected over a rather short period. As our focus is on multi-decadal variation, in the case where multiple change points are detected within 11-years, we choose the change point with the largest confidence level at the time when the trend has changed. In such cases, the trend change may actually take a few years in the real world.

The regression modelling based GAM is first carried out for the entire period of 1868/1869 winter to 2008/2009 winter, during which monthly *aa* are available. The same analysis is also carried out for the sub-periods separated by change points that are identified by the SMK test and by grouping the data into odd/even numbered SCs and/or ascending/declining phases of the SCs.

4. Results

4.1 Non-linear aa*-NAO relationship*

Fig. 1a shows the GAM fit of NAO_{DJFM} and aa_{DJFM} from 1869 to 2009 (where the years are defined by the January date). The smooth function f (see appendix 1) of the GAM fitting with an effective degree of freedom (EDF) equal to 2.5 (significant at the 0.05 level) indicates that there is statistical evidence of a nonlinear relationship between NAO_{DJFM} and aa_{DJFM} for the period of 1869-2009. Table 1 suggests that about 8% of the variance in NAO_{DJFM} may be explained by aa_{DJFM}. This *aa*-NAO relationship is marked by a non-linear concave shape in Fig. 1a with a negative relation for small to medium *aa* and a positive relation for medium to large *aa*. No significant linear model can be built between aa_{DJFM} and NAO_{DJFM} (see table 1). This result suggests that a nonlinear relationship is statistically

superior to the linear one for the entire period of 1869-2009. This is not only because the Akaike Information Criterion (AIC) [*Akaike*, 1974] of non-linear models is much lower compared to the corresponding AIC of the linear model (LM), but also because it is evident through the larger value of R^2.

On the other hand, no significant Rz -NAO relationship can be established by either linear or GAM models either for the period of 1825-2009 during which both the NAO_{DJFM} and Rz_{DJFM} were available (see Fig. 1b). No significant linear or non-linear Rz-NAO relationship can be established of the shorter common period of 1869-2009 either (not shown). Thus, at the interannual time scale, solar wind driven geomagnetic activity, rather than solar electromagnetic radiation or solar irradiance, is more likely to directly affect the winter NAO.

[Insert Fig. 1 here]

[Insert Table 1 here]

4.2 Multi-decadal Modulation by Solar Activity

Fig. 2a shows the time series of NAO_{DJFM} from 1825 to 2009. Fig. 2b shows the progressive ($U(t)$, the solid curve) and retrograde ($V(t)$, the dashed curve) scores of NAO_{DJFM} calculated by the SMK test. $U(t)$ and $V(t)$ cross each other around the winters 1907/1908, 1970/1971 and 1995/1996 (shown as red dashed vertical lines) where either $U(t)$ and $V(t)$ reaches or exceeds the confidence limits of 95% (blue dashed horizontal lines) before or after these crossing points. The crossing points indicate that a change in multi-decadal trend occurred at those times. Fig. 2b shows that there was no significant change in NAO_{DJFM} trend before 1907/1908. From 1908, NAO_{DJFM} started to decrease until 1970/1971 and then increase until 1995/1996. Since then, $U(t)$ and $V(t)$ cross each other frequently, implying a change of NAO_{DJFM} trend might have taken place over an extended period from 1996-2009.

It may also suggest that the NAO_{DJFM} trend has started to behave in a similar way to that in 1825-1880 during which period no significant trend was presented.

Fig. 2c shows the time series of aa_{DJFM} from 1869 to 2009. Fig. 2d shows that its progressive $U(t)$ and retrograde $V(t)$ scores do not cross each other at any time for the entire period, implying that no significant change of trend in aa_{DJFM} can be detected by SMK. A similar result is obtainable if the annual mean *aa* is used (not shown). Thus, over the extended period of 1869-2009, the long-term trend of the NAO is not statistically related to that of geomagnetic activity.

[Insert Fig. 2 here]

Fig. 3a;b show that the SMK-determined change points of the trend in the annual mean sunspot number Rz can be identified around 1812, 1844, 1903, and 1995 (black dashed vertical lines). The latter two change points of the Rz trend around 1903 and 1995 are remarkably close to those found in NAO_{DJFM} (shown as the red vertical lines taken from Fig. 2b). Thus, our results show that change points of the trend in Rz occur just before those in the NAO while the SMK test found no long-term connection between *aa* and the NAO (Fig 2d).

Although both annual and winter mean *aa* shows no significant change at multi-decadal time scale, it does have a statistically significant statistical inference on the winter mean NAO at shorter time-scales (*i.e.* interannual and decadal) according to the GAM (Fig. 1a). Conversely, winter mean sunspot number Rz shows no relationship with the NAO on an interannual time-scale but similar multi-decadal trend change points as the NAO. To resolve this issue we applied the SMK test to a 5-year running correlation (corr(*aa*, Rz)) between annual mean Rz and annual mean *aa* (see fig 3c). It shows that corr(*aa*, Rz) fluctuates with time. It has been suggested that the long-term variation in Rz and *aa* correlation may result

293 from a 40±50 year quasi-periodicity of the time lag between solar activity and geomagnetic
294 activity [*Echer et al.*, 2004; *Kishcha et al.*, 1999]. The rationale in the correlation between
295 Rz and *aa* used here is as a representation of the time varying response of the atmosphere to
296 geomagnetic activity in the presence of solar UV conditioning as previously found by *Lu et*
297 *al*. [2007]. Fig. 3d shows that significant change points of the trend in corr(*aa*, Rz) are also
298 found around 1903 and 1968 (Fig. 3c;d).

299 In addition, 1902 and 1957 are detected as significant change points of the trend of the
300 December to March mean sunspot area in the Sun's North Hemisphere (Fig. 3e;f), and 1963
301 and 1993 are found as significant change points of the trend of north-south asymmetry of
302 sunspot number As (Fig. 3g;h). A common feature of these change points of the trends of the
303 solar indices is that they all tend to precede the change points of NAO_{DJFM} by between 0 and
304 12 years. These results suggest that changes of solar activity at a multi-decadal scale might
305 have an effect on the change of the winter NAO trend.

306 **[Insert Fig. 3 here]**

307 In Fig. 4, we investigate the non-stationary behaviour of the *aa*-NAO relationship by
308 sub-dividing the datasets into the four periods identified by the SMK tests. As a general rule,
309 we chose to use those that represent the nearest change points to those detected in the NAO.
310 However, as most of the change points in the solar indices identified by the SMK tests were
311 around solar minimum except for the one around the 1960s to the 1970s, we chose to use
312 1962/1963 detected in solar asymmetry *As* rather than 1967/1968 detected in corr(*aa*, Rz) as
313 the separating years for the second and third periods. This is because 1963 was a solar
314 minimum year while 1968 was closer to the solar maximum of SC 20. Nevertheless, this
315 choice does not significantly change the conclusion in this paper.

316 Fig. 4 shows the GAMs fits for NAO_{DJFM} and aa_{DJFM} over the sub-periods of 1869-1902,
317 1903-1962, 1963-1995 and 1996-2009. The statistical measures of those models
318 corresponding to Fig. 4 are listed in Table 2 and compared with those from linear models
319 (LMs). From Table 2 and Fig. 4, it is evident from both linear and nonlinear models that the
320 *aa*-NAO relation changes with time. For the two end periods of 1869-1902 and 1996-2009,
321 no significant relationship between aa_{DJFM} and NAO_{DJFM} can be established. For the period
322 of 1903-1962, a significant negative linear realtion is found between NAO_{DJFM} and aa_{DJFM}.
323 Although this negative relationship is significant at the 0.01 level based on a LM, it may also
324 be described as weakly non-linear because slightly more of the variance in NAO_{DJFM} can be
325 explained by aa_{DJFM} when the GAM is used (R^2=0.17 for the GAM versus R^2=0.13 for the
326 LM) and smaller AIC value. Thus, we can say that 17% of the variance in the NAO_{DJFM} can
327 be explained by aa_{DJFM} during this period. For the period of 1963-1995, a significant positive
328 correlation is found between NAO_{DJFM} and aa_{DJFM}. The *aa*-NAO relationship for this sub-
329 period is significant at the 0.001 level based on a linear model (LM). Again, such a
330 relationship may also be described by a weak non-linear function because slightly more of the
331 variance in NAO_{DJFM} can be explained by aa_{DJFM} by using GAM (R^2=0.50 for the GAM
332 versus $R^2 = 0.42$ for the LM) and it produces a smaller AIC value. Thus we can say that 50%
333 of the variance of the NAO_{DJFM} can be explained by aa_{DJFM} during this period. These non-
334 linear concave shaped relationships remain significant at the 0.01 level, suggesting that the
335 negative and positive relationship in the second and third periods (*i.e.* 1903-1962 and 1963-
336 1995) contribute to form the overall concave-shaped *aa*-NAO relationship for the entire
337 period of 1869-2009 (see Fig. 1a). They further suggest that the *aa*-NAO relationship is not
338 stationary over the last 140 years and that multi-decadal variations of solar activity may be
339 linked to the non-stationary behaviour of the *aa*-NAO relationship.

340 **[Insert Fig. 4 here]**

[Insert Table 2 here]

4.3 Effect of Recurrent Solar Wind at different phases of the SC

In this section, we investigate the *aa*-NAO relationship by separating the data according to odd and even numbered SCs and then focus on the even numbered SCs, but separated by ascending and declining phases.

Fig. 5a shows how NAO_{DJFM} and aa_{DJFM} is grouped into odd (denoted by red circles) and even (denoted by black circles) numbered cycles while Fig.5b is the same as Fig. 1a except that the data belong to odd or even numbered solar cycles are colored differently. Fig. 5c shows that there is no statistical relationship between NAO_{DJFM} and aa_{DJFM} for the odd numbered SCs, while Fig. 5d suggests that there is significant *aa*-NAO relationship in even numbered SCs. It is worth noting that the concave-shaped relationship is nearly identical to the original one without any data separation (see Fig. 5b and Fig. 1a). However, by excluding the data from odd numbered solar cycles, the value of R^2 increases from 0.08 to 0.17 (see the first two rows of Table 3), which confirms that a non-linear relationship is again superior to the linear one. As a whole, results shown in Fig. 5 suggest that the non-linear *aa*-NAO is dominated by the data from the even numbered SCs.

[Insert Fig. 5 here]

[Insert Table 3 here]

Fig. 6 examines even numbered solar cycles in more detail. Fig. 6a shows how we sub-divided the data into ascending (red circles) and declining phases of even-numbered SCs. Fig. 6b is the same as Fig. 5d but with data colored differently for ascending and declining phases. Fig. 6c shows that there is an apparent non-linear relationship between NAO_{DJFM} and aa_{DJFM} for the ascending phase of even-numbered SCs. However, it is not statistically significant at the 0.05 level for the EDF (see the second last row of Table 3), so it may be coincidental. Fig.

365 6d shows that the concave-shaped *aa*-NAO relationship becomes clearer and more robust
366 statistically when only the data from the declining phase of even-numbered SCs are included.
367 Its concave-shape holds literally unchanged while it is significant at the 0.01 level compared
368 with 0.05 when data from the ascending phases are included (see Fig.6b and the second row
369 of table 3). It is worth noting that the value of R^2 increases from 0.17 to 0.34 when the data
370 from the ascending phases of even-numbered SCs were excluded (see table 3). This
371 represents 34% of the variances in the winter NAO under these conditions can be explained
372 by the geomagnetic *aa* index. A $R^2 = 0.34$ is about 4 times of its original value (0.08) where
373 all data for the entire period of 1869-2009 were used (see table 1). The progressive
374 improvement of R^2 and other statistical measures together with little alteration in the concave-
375 shaped relation strongly imply control of the data from the declining phase of even-numbered
376 SCs.

377 **[Insert Fig. 6 here]**

378 To further test the robustness of the winter *aa*-NAO relationship during the descending
379 phase of even-numbered SCs, we have used a bootstrap technique to assess the uncertainty of
380 the GAMs fitted to the *aa*-NAO relation. We have performed 10,000 bootstrap re-samplings
381 and built a GAM model for each sample. The re-sampling is done by sampling with
382 replacement and only the *aa* and the NAO data from the descending phase of even-numbered
383 SCs are used. Fig.7 shows that the mean fit of the 10,000 GAM bootstrapping models and the
384 associated uncertainty range are almost identical to those shown in Fig. 6(d). Thus, our
385 bootstrap analysis further confirms that the concave relationship holds firmly during the
386 descending phase of even-numbered solar cycles.

387 **[Insert Fig. 7 here]**

5. Discussions

Many large-scale atmospheric variables including global temperature and the NAO exhibit multi-decadal variations [*Boudouridis et al.*, 2003; *Delworth and Mann*, 2000; *Thompson et al.*, 2010]. However, little is known about what may have caused the multi-decadal variability [*Andronova and Schelsinger*, 2000; *Knight et al.*, 2006]. For the first time, we show that the geomagnetic effect on the winter NAO is non-stationary as well as non-linear. Its non-stationary behaviour is indicated by a decadal solar modulation of the shorter time scale relationship between geomagetic activity and the NAO. The multi-decadel variation in the NAO may be partially linked to long-term solar variation for the last 180 years as the changes of the NAO trend seemed to synchronize or follow those in solar activity. It is unknown what has caused the multi-decadal modulation. It might be attained by the solar UV effect on stratospheric ozone which, in turn, modulates the equator-to-pole temperature gradient in the stratosphere, which may modulate the atmospheric response to geomagnetic activity.

Changing behaviour of solar and/or geomagnetic activity has been reported before. *Clilverd et al.* [1998] show a significant enhancement of geomagnetic activity since the beginning of 1900s and suggested that the change was primarily caused by an increase in solar activity. *Stamper et al.* [1999] and *Lockwood et al.* [1999] suggested a doubling of Sun's coronal magnetic field during the 20th century.

While on decadal to interannual time-scales, a direct link between the NAO and the sunspot number cannot be found, there is however a weak but significant statistical connection between geomagnetic activity and the NAO over the period of 1869-2009. This indicates that on these shorter time scales, solar wind driven geomagnetic activity is more likely to affect the NAO than solar irradiance. This is consistent with the finding of *Woollings*

412 *et al*. [2010b] who showed a solar effect in the eastern part of the North Atlantic that was
413 much enhanced when open solar flux, rather than the F10.7 solar flux, was used to
414 characterize the 11-yr SC. *Barriopedro et al*. [2008] found that the 11-yr SC modulates the
415 preferred locations for high pressure blocking occurrence over the Atlantic Ocean where
416 blocking tends to be confined to either the western Atlantic under high solar conditions and
417 over eastern Atlantic under low solar conditions. Together, these results suggest that the solar
418 effect on the NAO is most likely of multiple sources operating on different time scales.

419 The fact that a non-linear *aa*-NAO relationship is dominated by the data from the
420 declining phase of even-numbered SCs suggests high speed recurrent solar wind streams may
421 be the cause of the *aa*-NAO relationship. It was observed that the largest contribution of
422 high-speed solar wind to auroral electron power tended to occur in the declining phases of the
423 SCs [*Cliver et al.*, 1996]. *Cliver et al.* [1996] found that the 22-year cycle in geomagnetic
424 activity is characterized by higher activity during the second half of even-numbered SCs and
425 the first half of odd-number cycles. Those authors suggested that a 22-year variation of
426 recurrent transient solar wind is due to cycle-to-cycle differences in the evolution of the
427 global magnetic field of the Sun. They also suggested that 27-day recurrent wind streams
428 were more prominent during the decline phase of even-numbered SCs, contributing to the
429 higher geomagnetic activity observed at those times. These stronger recurrence patterns may
430 be related to the more rapid expansion of polar coronal holes (faster movement of the coronal
431 streamer belt to low latitudes) observed following the maxima of recent even-numbered
432 cycles. Thus, the 22-year pattern of geomagnetic activity appears to be a reflection of the
433 solar dynamo coupling of poloidal magnetic fields during the decline phase of one solar cycle
434 to the toroidal fields at the maximum of the following cycle. This hypothesis has recently
435 been supported by *Shnirman et al*. [2009] and by *Georgieva and Kirov* [2010].

436 As shown in Fig. 8, there was a significant increase in geomagnetic activity in the period
437 from the beginning to the end of the 20th century, though a noticeable decrease of the daily *aa*
438 has been observed since the beginning of solar cycle 23. For the four sub-periods studied
439 here, 1963-1995 (blue dashed-dotted line) stands out to be the most active period with the
440 largest mean value and variance of the daily *aa*. The daily *aa* occurred significantly more
441 frequently for *aa* = 20 to 70 nT during 1963-1995 than during the sub-period1869-1902 (red
442 dashed line). For the extreme values of *aa* (*e.g*. daily *aa* > 80 nT), the differences between the
443 four sub-periods are small. As those extreme values of *aa* are mostly associated with CME
444 events while medium *aa* values are associated with CIR events, Fig. 8 further suggests that
445 the enhancement of geomagnetic activity during 1963-1995 is likely due to an increase of
446 high speed solar wind during this time period.

447 **[Insert Fig. 8 here]**

448 As shown in Fig. 9, the *aa*-NAO relationship becomes stronger and most significant
449 during the declining phases of even-numbered SC years for the sub-period 1963-1995 and
450 significantly weaker for other sub-periods. It is worth noting that, in Fig. 9a;d, there are three
451 outliers in 1969, 1995 and 1996; these were the years when the winter NAO values were
452 extreme and the solar indices were undergoing a change in their trends. Excluding those years
453 would significantly improve the *aa*-NAO relationship. For instance, for the sub-period 1963-
454 1995, the R^2 would increase from 0.59 to 0.92 and the *p*-value would decrease from 0.0008 to
455 1.67e-07 if the two outliers (*i.e*. 1969 and 1995) were excluded. It means that 59-92% of the
456 winter NAO variance can be explained by *aa* alone for the period of 1963-1995 and for those
457 years in the declining phases of even numbered SCs. As suggested by Fig. 8, the sub-period
458 1963-1995 stands out to be the most activity period in terms of high speed solar wind from
459 CIR events. In addition, 27-day recurrent wind streams are more prominent during the
460 decline of even-numbered solar cycles. Thus, the non-linear behaviour of the *aa*-NAO

461 relationship may be due to a threshold response of the winter NAO to geomagnetic forcing.
462 That is, such a detected geomagnetic effect on the NAO takes place only when there are
463 strong and persistent high speed solar wind streams emitted from the Sun. Below a certain
464 threshold value of geomagnetic forcing, the effect becomes too weak to be detected
465 statistically. This might be the reason that the significant positive correlation between *aa* and
466 the NAO only holds in 1970-1995 and collapsed before 1970 and after 1995, and why the
467 relationship becomes clearer when the data from the declining phases of even-numbered SCs
468 only are included.

469 **[Insert Fig. 9 here]**

470 The fact that the *aa*-NAO relationship is dominated by the even numbered SC may also
471 be related to the Rosenberg-Coleman (RC) effect [*Rosenberg and Coleman*, 1969]. The
472 rotation axis of the Sun is tilted 7° with respect to the ecliptic plane so that near the spring
473 equinox in March the Earth is at maximum southern heliographic latitudes and near the
474 equinox in September it is at maximum northern heliographic latitudes. *Rosenberg* and
475 *Coleman* [1969] discovered that the dominant polarity of the IMF at times of most exposure
476 to northern and southern latitudes is the same as the polarity of the corresponding pole on the
477 Sun. Thus when the northern pole of the Sun is positive the IMF is away from the Sun above
478 the heliographic equator. The Earth is above the Sun's equator around September and
479 according to the RC effect will be dominated by IMF pointing away from the Sun. According
480 to the RM rule [*Russell and McPherron*, 1973], this is a geo-effective orientation as it
481 represents the most suitable IMF sector structure. Six months later the Earth will be at high
482 southern latitudes where the IMF is toward the Sun. This situation is also geo-effective. Thus
483 throughout an 11-year SC the ordinary behaviour of the IMF is conducive to the production
484 of variations in geomagnetic activity. However, it remains unclear why the *aa*-NAO
485 relationship is particularly strong during the declining phases of the even-numbered solar

cycles though it seems to link to persistent high speed solar wind streams. More research is needed to clarify the underlying reasons for the dominant role of the declining phases of even-numbered SC in order to establish the observed *aa*-NAO relationship.

It remains to be understood why the *aa*-NAO relationship switches from a negative effect for small to medium *aa* and a positive one for medium to large *aa*. It might be due to the way that the geomagnetic forcing is coupled with Earth's atmosphere circulation and it may be producing a shift in atmospheric circulation. The presence of the solar UV conditioning as previously found by *Lu et al*. [2007] may also play a role in the solar modulation of the *aa*-NAO relationship at the multi-decadal scale. To make the matter even more complicated, the connection between the 11-yr SC and atmospheric variables can be further modulated by atmospheric internal variability such as the stratospheric Quasi-biennial Oscillation [e.g. *Labitzke*, 1987; *Lu et al*., 2009].

6. Conclusions

In this study, we have re-examined the statistical relationship between geomagnetic activity and the winter NAO. Our results indicate that a significant relationship can be established, which can be generally described by non-linear concave shape with a negative relation for small to medium *aa* and a positive relation for medium to large *aa*. The finding that the *aa*-NAO relationship is also non-stationary such that it may be ascribed a multi-decadal modulation of solar activity. A multi-decadal modulation of the winter time *aa*-NAO relationship by solar activity signifies that the Sun is more likely to affect Earth's climate by multiple means and the effects of solar and geomagnetic activity take place with different time-scales. Thus, the Sun-Climate connection is best viewed as a non-linear and non-stationary process.

509 The dominant role of the declining phases of even-numbered SCs in the *aa*-NAO
510 relationship indicates that the 27-day recurrent solar wind streams may be responsible for
511 the observed *aa*-NAO relationship. It is also possible that an increase of long-duration
512 recurrent solar wind streams from high latitude coronal holes during solar cycles 20 and 22
513 may partially account for the significant positive *aa*-NAO relationship during the latter third
514 of the 20th century.

515 More detailed studies are required to understand how the geomagnetic activity may
516 affect the stratospheric and tropospheric circulation and wave activity, how those changes
517 are communicated downward to influence the North Atlantic region, and to what extent the
518 effect seen in our statistical analysis may be linked to known mechanisms such as energetic
519 particle precipitation induced NOx [*Randall et al.*, 2005; *Solomon et al.*, 1982] and longer-
520 term changes in stratosphere ozone [*Haigh*, 1994].

521

522 *Acknowledgements*: YL and BB were supported by the Indian Ocean Climate Initiative.
523 HL, MJJ and MAC were supported by the UK Natural Environment Research Council
524 (NERC). We thank two anonymous reviewers for their constructive comments.

Appendix 1: Generalized Additive Model

The Generalized Additive Model (GAM) is a nonparametric modelling technique that objectively estimates the functional relationship between the predictand and predictors in an additive model. In this study, we only consider a univariate model for detecting the relationship between a continuous predictand Y_t (*e.g.*, the NAO) and a predictor X_t (*e.g.*, the *aa* index). As a result, the GAM fits a univariate regression model between the predicant Y_t and predictor X_t,

$$Y_t = \beta_0 + f(X_t) + \varepsilon_t \quad (1)$$

where f is an unspecified smooth function to be estimated from observed data $\{(X_t, Y_t) : t = 1,2,\ldots,n\}$, β_0 is the constant (or intercept) and ε_t the residual which follows a Gaussian distribution with zero mean and a constant variance. Note the error distribution may be relaxed to include not only a Gaussian, but all distributions from the exponential family (binomial, Poisson and Gamma). Here the error is assumed to follow a Gaussian distribution because the predicant (*i.e.* the NAO) is approximately Gaussian.

There are several ways of defining the smooth function $f(X_t)$ and *Hastie and Tibshirani* [1990] give a useful overview of different types of smoothers. Here we use Wood's methods based on penalized regression smoothers [*Wood*, 2006]. Specifically, the smooth function $f(X_t)$ used in this study is of the form

$$f(X_t) = \sum_{i=1}^{M} b_i(X_t)\beta_i \quad (2)$$

where $b_i(X_t)$ are a set of cubic spline basis functions with $b_1(X_t) = X_t$ and $b_i(X_t) = |X_t - X_i^*|^3$ for $i = 2,\ldots,M$, $\{X_i^* : j = 2,\ldots,M\}$, and β_i are the parameters to be estimated. Note that X_i are a set of points in the range of X_t known as the "knots" of the spline and M is the basis dimension (*i.e.* the number of basis functions). Increasing M allows

550 $f(X_t)$ to track the data more closely while decreasing M makes $f(X_t)$ to become more
551 linear. For instance, substituting (2) into (1) with $M = 1$ yields a linear model.
552 Part of the GAM fitting process is to choose the appropriate degree of smoothness.
553 Wood's method includes a penalty term in the model likelihood. This penalty term is
554 controlled by a smoothing parameter λ which determines the trade-off between the goodness
555 of fit of the model and its smoothness. If $\lambda = 0$, meaning there is no smoothing, it is
556 equivalent to fitting the model using its original basis dimension. As $\lambda \to \infty$, there is a large
557 amount of smoothing, which would result in a similar effect of choosing a lower basis
558 dimension M. The smoothing parameter λ is selected to minimize the generalized cross
559 validation score (GCV) [*Craven and Wabha*, 1979].
560 Given the estimated smooth parameter λ, and the basis dimension *M*, the effective degree
561 of freedom (EDF) for the smooth function $f(X_t)$ can be calculated. The EDF will be in the
562 range of $[1, M]$ and is a measure of the complexity of the contribution of X_t to $f(X_t)$ in
563 the form of eq. (1). That is, $f(X_t)$ with EDF=1 represents a straight-line relationship and
564 could be replaced by a liner term βX_t. As the EDF approaches M the relationship is more
565 complex. The smooth function $f(X_t)$ therefore gives the ability to examine the relationship
566 between the predictand Y_t and predictor X_t, whether they are linearly or non-linear related.
567 The "data-driven" estimated $f(X_t)$ is therefore most helpful to describe the unknown
568 relationship between the predictand Y_t and predictor X_t when there is no prior knowledge
569 [*Underwood*, 2009].
570 Whether or not a fitted model is better or worse than another is determined by the Akaike
571 Information Criterion (AIC) test statistic [*Akaike*, 1974]. AIC is a function of both the log

likelihood function and the effective number of parameters being estimated [*O'Brien et al.*, 1996]. For a GAM with EDF = k, the AIC is calculated as

$$\mathrm{AIC} = D + 2k\phi$$

where D is the deviance and ϕ is the dispersion parameter (variance). The deviance estimated in the model, analogous to the residual sums of squares, is a measure of the fit of the model. A pseudo coefficient of determination, R^2, is estimated as 1.0 minus the ratio of the deviance of the model to the deviance of the null model [*Swartzman et al.*, 1992]. It is worth noting that the pseudo R^2, is equivalent to the R^2 for the models fitted with Gaussian error model. In this case, the deviance of the null model corresponds to the sum of total squares. Thus, the pseudo R^2 is defined as the proportion of variation in Y_t accounted for by the fitted model.

Note that a linear model is nested within a GAM. The inference about the nonlinearity of the effect of a predictor is therefore accomplished by an analysis of deviance. Specifically, the nonlinearity of the effect of a given predictor (*e.g.* the *aa* index) is tested by comparing the deviance of the k degrees of freedom (df) smoothed model to the deviance of a 1-df linear model [*Hastie and Tibshirani*, 1990]. The resulting non-parametric likelihood ratio test statistic is approximately distributed as a χ^2 statistic with $k-1$ dfs, which can be used to test the significance of the nonlinearity of $f(X_t)$ in terms of its EDF significantly bigger than 1 [*Hastie and Tibshirani*, 1990].

A R package named *mgcv* [*Wood*, 2006] provides easy access to the GAM technique described briefly above. *Wood* [2006] has also provided further detailed introduction, explanation and description of this method. The most recent development of this method is also available in the updated *mgcv* package [*Wood*, 2008].

595 All modeling results including AIC, EDF and R^2, and the significance of the nonlinearity
596 of $f(X_t)$ in this study were obtained by using the *mgcv* package, and are given in Table 1-3.

597

598 ***Appendix 2: Sequential Mann-Kendall test***
599

600 The sequential Mann-Kendall (SMK) test is a statistical technique to determine potential
601 trend change in a time series. Following *Gerstengarbe and Werner* [1999], let a time series
602 $\mathbf{X} = \{X_1, \ldots, X_n\}$ be separated into $n-1$ subseries (i.e. the first subseries includes the sample
603 values X_1, X_2, the second include the values X_1, X_2, X_3 etc). The $n-1$ Mann-Kendall test
604 statistic variables [*Mann*, 1945] determined by these subseries are given as:

605 $$W_t = \sum_{i=1}^{t} R_i$$

606

607 where R_i is the rank of the *t-th* subseries $\{X_1, X_2, \cdots, X_{t+1}\}$, *i.e.*, the number of the elements
608 $X_i (i > j)$ such that $X_i > X_j$ with $i = 2, \ldots, t$ and $j = 1, \ldots, i-1$. Consequently, for each of the
609 $n-1$ subseries, the corresponding progressive row $U(t)$ is defined as

610 $$U(t) = \frac{W_t - E(W_t)}{\sqrt{Var(W_t)}}$$

611 where $E(W_t)$ is the expected value of the respective subseries with

612 $$E(W_t) = \frac{l_t(l_t - 1)}{4}$$

613 and $Var(W_t)$ is the respective variance given by

614 $$Var(W_t) = \frac{l_t(l_t - 1)(2l_t - 5)}{72}$$.

For $l_t \to \infty$ (l_t = the length of the subseries), W_t is approximately Gaussian [see *Gerstengarbe and Werner*, 1999] and the normalized $U(t)$ is assumed to be a standard Gaussian distribution. Similarly, the test statistic variable $V(t)$ can be defined and calculated by using the corresponding rank series for the so-called retrograde rows for the resorted sample $\{X_{t+1}, X_t, \cdots, X_1\}$ for $t = 1, \ldots, n-1$.

After the test statistic variables $U(t)$ and $V(t)$ are calculated for all progressive and retrograde series, one obtains $n-1$ corresponding values of so-called the progressive and retrograde rows, respectively. Points where the two rows of $U(t)$ and $V(t)$ cross are considered as potential trend turning points within the time series. When either the progressive $U(t)$ or retrograde $V(t)$ row exceeds certain confidence limits before and after the crossing point, the null hypothesis (the sampled time series has no change points) must be rejected, and this trend turning point is considered significant at the corresponding level, *i.e.* 1.96 for 95% significant level.

628

629 ## References

630

631 Akaike, H. (1974), New Look at Statistical-Model Identification, *IEEE Transactions on Automatic*
632 *Control*, *Ac19*(6), 716-723.
633 Andronova, N. G., and M. E. Schelsinger (2000), Causes of global temperature changes during the
634 19th and 20th centuries., *Geophys. Res. Lett.* , *27*, 2137-2140.
635 Arnold, N. F., and T. R. Robinson (2001), Solar magnetic flux influences on the dynamics of the winter
636 middle atmosphere, *Geophys. Res. Lett.*, *28*(12), 2381-2384.
637 Badalyan, O.G. and V.N. Obridko (2011), North–South asymmetry of the sunspot indices and its
638 quasi-biennial oscillations, *New Astronomy*, 16, 357-365.Barriopedro, D., R. Garćıa-Herrera,
639 and R. Huth (2008), Solar modulation of Northern Hemisphere winter blocking, *J. Geophys. Res.*,
640 *113*, D14118, doi:14110.11029/12008JD009789.
641 Boberg, F., and H. Lundstedt (2002), Solar wind variations related to fluctuations of the North
642 Atlantic Oscillation, *Geophys. Res. Lett.*, *29*(15), 1718, 1710.1029/2002GL014903.
643 Boberg, F., and H. Lundstedt (2003), Solar wind electric field modulation of the NAO: A correlation
644 analysis in the lower atmosphere, *Geophys. Res. Lett.*, *30*(15), 1825,
645 doi:1810.1029/2003GL017360.
646 Bochnicek, J., and P. Hejda (2005), The winter NAO pattern changes in association with solar and
647 geomagnetic activity, *J. Atmos. Sol.-Terr. Phys.*, *67*, 17-32.
648 Boudouridis, A., E. Zesta, L. R. Lyons, P. C. Anderson, and D. Lummerzheim (2003), Effect of soalr
649 wind pressure pulses on the size and strength of the auroral oval, *J. Geophys. Res.*, *108*, A8012,
650 doi:8010.1029/2002JA009373.
651 Bucha, V., and V. Bucha (1998), Geomagnetic forcing of changes in climate and in the atmospheric
652 circulation, *J. Atmos. Sol.-Terr. Phys.*, *60*(2), 145-169.
653 Bumba, V., and L. Hejna (1991), A new index of recurrence for long-lasting enhanced geomagnetic
654 activity, *Bull. Astron. Inst. Czech.*, *42*(2), 85-90.
655 Clilverd, M. A., T. D. G. Clark, E. Clarke, and H. Rishbeth (1998), Increased magnetic storm activity
656 from 1868 to 1995, *J. Atmos. Sol.-Terr. Phys.*, *60*(10), 1047-1056.
657 Cliver, E. W., V. Boriakoff, and K. H. Bounar (1996), The 22-year cycle of geomagnetic and solar wind
658 activity, *J. Geophys. Res.*, *101*(A12), 27,091–027,109, doi:010.1029/1096JA02037.
659 Corti, S., F. Molteni, and T. N. Palmer (1999), Signature of recent climate change in frequencies of
660 natural atmospheric circulation regimes, *Nature*, *398*, 799-802.

661 Cox, M. E., A. Moss, and G. K. Smyth (2005), Water quality condition and trend in North Queensland
662 waterways, *Marine Pollution Bulletin*, *51*(1-4), 89-98.
663 Craven, P., and G. Wahba (1979), Smoothing noisy data with spline functions. *Numer. Math. 31*(4),
664 377-403.
665 Delworth, T. L., and M. E. Mann (2000), Observed and simulated multidecadal variability in the
666 Northern Hemisphere, *Clim. Dyn.* , *16*, 661–676.
667 Echer, E., W. D. Gonzalez, A. L. C. Gonzalez, A. Prestes, L. E. A. Vieira, A. Dal Lago, F. L. Guarnieri, and
668 N. J. Schuch (2004), Long-term correlation between solar and geomagnetic activity, *J. Atmos.*
669 *Sol.-Terr. Phys.*, *66*(12), 1019–1025.
670 Emery, B. A., I. G. Richardson, D. S. Evans, and F. J. Rich (2009), Solar wind structure sources and
671 periodicities of auroral electron power over three solar cycles, *J.Atoms.Sol.-Terr.Phys.*, *71*, 1157-
672 1175.
673 Enfield, D. B., A. M. Mestas-Nuñez, and P. J. Trimble (2001), The Atlantic Multidecadal Oscillation and
674 its relation to rainfall and river flows in the continental US, *Geophys. Res. Lett.*, *28*, 2077-2080.
675 Feldstein, S. B. (2002), The recent trend and variance increase of the annular mode, *J. Clim.*, *15*, 88-
676 94.
677 Georgieva, K., and B. Kirov (2010), Solar dynamo and geomagnetic activity, *J. Atmos. Sol.-Terr. Phys.*.,
678 doi:10.1016/j.jastp.2010.03.003.
679 Gerstengarbe, F. W., and P. C. Werner (1999), Estimation of the beginning and end of recurrent
680 events within a climate regime, *Clim. Res.*, *11*, 97-107.
681 Gillett, N. P., F. W. Zwiers, A. J. Weaver, and P. A. Stott (2003), Detection of human influence on sea-
682 level pressure, *Nature*, *422*(6929), 292-294.
683 Gong, G., D. Entekhabi, and J. Cohen (2002), A Large-ensemble model study of the wintertime AO–
684 NAO and the role of interannual snow perturbations, *J. Clim.*, *15*, 3488-3499.
685 Gong, G., D. Entekhabi, and J. Cohen (2003), Modeled Northern Hemisphere winter climate response
686 to realistic Siberian snow anomalies, *J. Clim.*, *16*, 3917-3931.
687 Gray, S. T., L. J. Graumlich, J. L. Betancourt, and G. T. Pederson (2004), A tree-ring based
688 reconstruction of the Atlantic Multidecadal Oscillation since 1567 A.D. , *Geophys. Res. Lett.* , *31*,
689 L12205.
690 Gu, C. (2002), Cross-validating non-Gaussian data, *J. Comput. Graph. Stat.*, *1*, 169-179.
691 Haigh, J. D. (1994), The role of stratospheric ozone in modulating the solar radiative forcing of
692 climate, *Nature*, *370*(6490), 544-546.
693 Hall, A., and M. Visbeck (2002), Synchronous variability in the southern hemisphere atmosphere, sea
694 ice, and ocean resulting from the annular mode, *J. Clim.*, *15*(21), 3043-3057.

695 Hapgood, M. A. (1993), A double solar cycle in the 27-day recurrence of geomagnetic activity, *Ann.*
696 *Geophys.*, *11*, 248-253.
697 Harrison, R. G., and D. B. Stephenson (2006), Empirical evidence for a nonlinear effect of galactic
698 cosmic rays on clouds, *Proc. R. Soc. London, Ser. A*, *462*(2068), 1221-1223,
699 doi:10.1098/rspa.2005.1628.
700 Hastie, and R. Tibshirani (1990), Generalized Additive Models, *Chapman and Hall*.
701 He, S., S. Mazumdar, and V. C. Arena (2006), A comparative study of the use of GAM and GLM in air
702 pollution research, *Environmetrics*, *17*(1), 81-93.
703 Hoerling, M. P., J. W. Hurrell, and T. Y. Xu (2001), Tropical origins for recent North Atlantic climate
704 change, *Science*, *292*(5514), 90-92.
705 Hurrell, J. W. (1995), Decadal trends in the North-Atlantic Oscillation - Regional temperatures and
706 precipitation, *Science*, *269*(5224), 676-679.
707 Hurrell, J. W., and C. Deser (2010), North Atlantic climate variability: The role of the North Atlantic
708 Oscillation, *J. Marine Syst.*, *79*, 231-244.
709 Hurrell, J. W., Y. Kushnir, G. Ottersen, and M. E. Visbeck (2003), *The North Atlantic Oscillation:*
710 *Climate Significance and Environmental Impact*, 279pp pp., AGU Geophysical Monograph.
711 Iman, R. L. (1994), *A Data-Based Approach to Statistics*, 348 pp., Duxbury, Pacific Grove, Calif.
712 Jones, P. D., T. Jónsson, and D. Wheeler (1997), Extension to the North Atlantic Oscillation using
713 early instrumental pressure observations from Gibraltar and South-West Iceland, *Int. J.*
714 *Climatol.* , *17*, 1433-1450.
715 Kishcha, P. V., I. V. Dmitrieva, and V. N. Obridko (1999), Long-term variations of the solar-
716 geomagnetic correlation, total solar irradiance, and northern hemispheric temperature
717 (1868±1997), *J. Atmos. Sol.-Terr. Phys.*, *61*, 799-808.
718 Knight, J. R., C. K. Folland, and A. A. Scaife (2006), Climate impacts of the Atlantic Multidecadal
719 Oscillation, *Geophys. Res. Lett.* , *33*, L17706.
720 Kniveton, D. R., B. A. Tinsley, G. B. Burns , E. A. Bering , O.A. Troshichev (2008), Variations in global
721 cloud cover and the fair-weather vertical electric field, *J. Atmos. Sol.-Terr. Phys*., *70*, 1633-
722 1642.
723 Kodera, K. (2002), Solar cycle modulation of the North Atlantic Oscillation: Implication in the spatial
724 structure of the NAO, *Geophys. Res. Lett.*, *29*(8), 1218, doi:1210.1029/2001GL014557.
725 Kodera, K. (2003), Solar influence on the spatial structure of the NAO during the winter 1900-1999,
726 *Geophys. Res. Lett.*, *30*(4), 1175 doi:1110.1029/2002GL016584.
727 Labitzke K. (1987), Sunspots, the QBO, and the stratospheric temperature in the north polar-region,
728 *Geophys. Res. Lett*., *14*, 535-537.

729 Laken, B., A. Wolfendale, and D. Kniveton (2009), Cosmic ray decreases and changes in the liquid
730 water cloud fraction over the oceans, *Geophys. Res. Lett*., *36*, L23803,
731 doi:10.1029/2009GL040961.
732 Li, K. J., J. X. Wang, S. Y. Xiong, H. F. Liang, H. S. Yun and X. M. Gu (2002), Regularity of the north-
733 south asymmetry of solar activity, Astronomy & Astrophysics, *383*(2), 648-652, Doi:
734 10.1051/0004-6361:20011799.
735 Liu, Y., C. J. Paciorek, and P. Koutrakis (2009), Estimating Regional Spatial and Temporal Variability of
736 PM2.5 Concentrations Using Satellite Data, Meteorology, and Land Use Information, *Environ.*
737 *Health Persp.*, *117*(6), 886-892.
738 Lockwood, M., R. Stamper, and M. N. Wild (1999), A doubling of the Sun's coronal magnetic field
739 during the last 100 years, *Nature*, *399*, 437-439.
740 Lu, H., M. A. Clilverd, A. Seppälä, and L. L. Hood (2008a), Geomagnetic perturbations on
741 stratospheric circulation in late winter and spring, *J. Geophys. Res.*, *113*, D16106,
742 doi:16110.11029/12007JD008915.
743 Lu, H., L. J. Gray, M. P. Baldwin, M. J. Jarvis (2009), Life cycle of the QBO-modulated 11-year solar
744 cycle signals in the Northern Hemispheric winter. *Q. J. R. Meteorol. Soc.*, 135, 1030-1043.
745 Lu, H., M. J. Jarvis, R. E. Hibbins (2008b), Possible solar wind effect on the Northern Annular Mode
746 and northern hemispheric circulation during winter and spring, *J. Geophys. Res.*, *113*, D23104,
747 doi:10.1029/12008JD010848.
748 Lu, H., M. J. Jarvis, H. F. Graf, P. C. Young, and R. B. Horne (2007), Atmospheric temperature
749 response to solar irradiance and geomagnetic activity, *J. Geophys. Res.*, *112*, D11109,
750 doi:11110.11029/12006JD007864.
751 Mann, H.B. (1945) Non parametric test against trend. *Econometric*, *13*, 245-259.
752 Mayaud, P. N. (1972), The *aa* indices: a 100-year series characterising the magnetic activity, *J.*
753 *Geophys. Res.*, *72*, 6870-6874.
754 McLeod, S. R., and A. R. Pople (2010), Modelling the distribution and relative abundance of feral
755 camels in the Northern Territory using count data, *Rangeland J.*, *32*(1), 21-32.
756 Mehta, V. M., M. J. Suarez, J. V. Manganello, and T. L. Delworth (2000), Oceanic influence on the
757 North Atlantic Oscillation and associated Northern Hemisphere climate variations: 1959-1993,
758 *Geophys. Res. Lett.*, *27*(1), 121-124.
759 Mestre, O., and S. Hallegatte (2009), Predictors of Tropical Cyclone Numbers and Extreme Hurricane
760 Intensities over the North Atlantic Using Generalized Additive and Linear Models, *J. Clim., 22*(3),
761 633-648.

762 Mikolajczyk, R. T., A. E. Maxwell, W. El Ansari, C. Stock, J. Petkeviciene, and F. Guillen-Grima (2010),
763 Relationship between perceived body weight and body mass index based on self- reported
764 height and weight among university students: a cross-sectional study in seven European
765 countries, *BMC Public Health*, *10*:40 doi:10.1186/1471-2458-10-40.
766 Morton, R., and B. L. Henderson (2008), Estimation of nonlinear trends in water quality: An improved
767 approach using generalized additive models, *Water Resour. Res.*, 44, W07420,
768 doi:10.1029/2007WR006191. Ogi, M., K. Yamazaki, and Y. Tachibana (2003), Solar cycle
769 modulation of the seasonal linkage of the North Altantic Oscillation (NAO), *Geophys. Res. Lett.*,
770 *30*(22), 2170, doi: 2110.1029/2003GL018545.
771 Osborn, T. J. (2004), Simulating the winter North Atlantic Oscillation: the roles of internal variability
772 and greenhouse gas forcing, *Clim. Dyn.* , *22*(6-7), 605-623.
773 Palamara, D. R., and E. A. Bryant (2004), Geomagnetic activity forcing of the Northern Annular Mode
774 via the stratosphere, *Ann. Geophys.*, *22*, 725-731.
775 Paluš, M., and D. Novotná (2007), Common oscillatory modes in geomagnetic activity, NAO index
776 and surface air temperature records, *J. Atmos. Sol.-Terr. Phys.*, *69*, 2405-2415
777 Paluš, M., and D. Novotná (2009), Phase-coherent oscillatory modes in solar and geomagnetic
778 activity and climate variability, *J. Atmos. Sol.-Terr. Phys.*, *71*, 923-930.
779 Pierce, J. R., and P. J. Adams (2009), Can cosmic rays affect cloud condensation nuclei by altering
780 new particle formation rates?, *Geophys. Res. Lett*., *36*, L09820, doi:10.1029/2009GL037946.
781 Press, W. H., B. P. Flannery, S. A. Teukolsky, and W. T. Vetterling (1992), *Numerical Recipes in C: The*
782 *Art of Scientific Computing,* 2nd ed., 848 pp., Cambridge Univ. Press, New York.
783 Pudovkin, M. I., and S. V. Veretenenko (1995), Cloudiness decreases associated with Forbush-
784 decreases of galactic cosmic rays, *J. Atmos. Sol. Terr. Phys*., *57*(11), 1349-1355,
785 doi:10.1016/0021-9169(94)00109-2.
786 Pudovkin, M. I. and S. V, Veretenenko (1996), Variations of the cosmic rays as one of the possible
787 links between the solar activity and the lower atmosphere, *Adv. Space Res*., *17*(11), 161-164.
788 Randall, C. E., V. L. Harvey, C. S. Singleton, P. F. Bernath, C. D. Boone, and J. U. Kozyra (2006),
789 Enhanced NOx in 2006 linked to strong upper stratospheric Arctic vortex, *Geophys. Res. Lett.*,
790 *33*, L18811, doi:18810.11029/12006GL027160.
791 Randall, C. E., V. L. Harvey, C. S. Singleton, S. M. Bailey, P. F. Bernath, M. Codrescu, H. Nakajima, and
792 J. M. Russell III (2007), Energetic particle precipitation effects on the Southern Hemisphere
793 stratosphere in 1992–2005, *J. Geophys. Res.*, *112*, D08308, doi:08310.01029/02006JD007696.
794 Randall, C. E., et al. (2005), Stratospheric effects of energetic particle precipitation in 2003-2004,
795 *Geophys. Res. Lett*., *32*(5), L05802, doi:05810.01029/02004GL022003.

796 Rangarajan, G. K. (1991), Variations in the strength of recurrent geomagnetic activity in solar cycles
797 11 to 21, *J. Earth Planet. Sci. (Proc. Indian Acad. Sic.)*, *100,* 49-54.
798 Rodwell, M. J., D. P. Rowell, and C. K. Folland (1999), Oceanic forcing of the wintertime North
799 Atlantic Oscillation and European climate, *Nature*, *398*(6725), 320-323.
800 Rosenberg, R., and P. J. Coleman (1969), Heliographic latitude dependence of the dominant polarity
801 of the interplanetary magnetic field, *J. Geophys. Res.*, *74*(24), 5611-5622.
802 Russell, C.T., and R.L. McPherron (1973), Semiannual variation of geomagnetic activity, *J. Geophys.*
803 *Res. 78*(1), 92-108.
804 Saenger, C., A. L. Cohen, D. W. Oppo, R. B. Halley, and J. E. Carilli (2009), Surface-temperature trends
805 and variability in the low-latitude North Atlantic since 1552, *Nature Geoscience*, *2*, 492-495.
806 Sargent, H. H., III, (1985), Recurrent geomagnetic activity: Evidence for long-lived stability in solar
807 wind structure, *J. Geophys. Res.*, *90*(A2), 1425–1428, doi:1410.1029/JA1090iA1402p01425.
808 Sargent, H. H., III, (1986), The 27-day recurrence index, in: *Solar Wind Magnetosphere Coupling*,
809 edited by Y. Kamide and J. A. Slavin, p. 143, Terra Sci., Tokyo.
810 Seppälä, A., C. E. Randall, M. A. Clilverd, E. Rozanov, and C. J. Rodger (2009), Geomagnetic activity
811 and polar surface air temperature variability, *J. Geophys. Res.*, *114*, A10312,
812 doi:10310.11029/12008JA014029.
813 Shaviv, N. J. (2005), On climate response to changes in the cosmic ray flux and radiative budget, *J.*
814 *Geophys. Res.*, *110*, A08105, doi:08110.01029/02004JA010866.
815 Shindell, D. T., R. L. Miller, G. A. Schmidt, and L. Pandolfo (1999), Simulation of recent northern
816 winter climate trends by greenhouse-gas forcing, *Nature*, *399*(6735), 452-455.
817 Shnirman, M. G., J.-L. L. Mouël, and E. M. Blanter (2009), The 27-day and 22-year cycles in solar and
818 geomagnetic activity, *Solar. Phys.*, *258*(1), 167-179, DOI: 110.1007/s11207-11009-19395-11209.
819 Sneyers, R. (1990), *On statistical analysis of series of observations*. 143pp, World Meteorological
820 Society, Geneva, Switzerland.
821 Solomon, S., P. J. Crutzen, and R. G. Roble (1982), Photochemical coupling between the
822 thermosphere and the lower atmosphere: 1. Odd nitrogen from 50 to 120 km, *J. Geophys. Res.*,
823 *87*, 7206-7220.
824 Stamper, R., M. Lockwood, and M. N. Wild (1999), Solar causes of the long-term increase in
825 geomagnetic activity, *J. Geophys. Res.*, *104*(A12), 28325-28342.
826 Stephenson, D. B., V. Pavan, and R. Bojariu (2000), Is the North Atlantic Oscillation a random walk?,
827 *Int. J. Climatol.*, *20*, 1-18.

828 Svensmark, H., and E. Friis-Christensen (1997), Variation of cosmic ray flux and global cloud
829 coverage: A missing link in solar-climate relationships, *J. Atmos. Sol. Terr. Phys*., *59*(11), 1225–
830 1232, doi:10.1016/S1364- 6826(97)00001-1.
831 Svensmark, H., T. Bondo, and J. Svensmark (2009), Cosmic ray decreases affect atmospheric aerosols
832 and clouds, *Geophys. Res. Lett*., *36*, L15101, doi:10.1029/2009GL038429.
833 Swartzman, G., C. H. Huang, and S. Kaluzny (1992), Spatial-Analysis of Bering Sea Groundfish Survey
834 Data Using Generalized Additive-Models, *Can J Fish Aquat Sci*, *49*(7), 1366-1378.
835 Taubenheim, J. (1989), An easy procedure for detecting a discontinuity in a digital time series. *Z*.
836 *Meteorol*., *39*(6), 344-347.
837 Thejll, P., B. Christiansen, and H. Gleisner (2003), On correlations between the North Atlantic
838 Oscillation, geopotential heights, and geomagnetic activity, *Geophys. Res. Lett.*, *30*(6), L1347,
839 doi:1310.1029/2002GL016598.
840 Thompson, D. W. J., J. M. Wallace, J. J. Kennedy, and P. D. Jones (2010), An abrupt drop in Northern
841 Hemisphere sea surface temperature around 1970, *Nature*, *467*, 444-447.
842 Tinsley, B. A., G. B. Burns, and L. Zhou (2007), The role of the global electric circuit in solar and
843 internal forcing of clouds and climate. *Adv. Space Res*., *40*, 1126-1139.
844 Underwood, F.M (2009), Describing long-term trends in precipitation using generalized additive
845 models. *J. Hydrol., 364*, 285-297.
846 Wood, S. N. (2006), Generalized Additive Models: An Introduction with R, Chapman and Hall/CRC.
847 Wood, S. N. (2008), Fast stable direct fitting and smoothness selection for generalized additive
848 models, *J. Roy. Stat. Soc.* ***B***, *70*, 495-518.
849 Woollings, T., A. Hannachi, B. Hoskins, and A. Turner (2010a), A regime view of the North Atlantic
850 Oscillation and its response to anthropogenic forcing, *J. Clim.*, Doi: 10.1175/2009JCLI3087.1171.
851 Woollings, T., M. Lockwood, G. Masato, C. Bell, and L. Gray (2010b), Enhanced signature of solar
852 variability in Eurasian winter climate, *Geophys. Res. Lett.*, *37*, L20805,
853 doi:20810.21029/22010GL044601.

Figure captions:

Fig. 1: (a): scatter plot of the December to March mean NAO_{DJFM} against the December to March mean geomagnetic *aa* index aa_{DJFM} from the period of 1869-2009. (b): scatter plot of NAO_{DJFM} against the December to March mean sunspot number Rz_{DJFM} from the period of 1825-2009. The black lines denote the GAM fitting while the shaded region shows the 95% confidence interval for GAM model. When the output of the GAM is linear, only the linear model and its 95% confidence interval are shown. The small vertical bars inside of the *x*-axis represent the corresponding values of Rz_{DJFM} and aa_{DJFM} for all the samples.

Fig. 2: (a;c): time evolution of NAO_{DJFM} and aa_{DJFM} for the period of 1800-2009. Note that aa_{DJFM} started from 1869 while NAO_{DJFM} started from 1825. (b;d): the progressive ($U(t)$, solid) or retrograde ($V(t)$, dashed) scores of NAO_{DJFM} and aa_{DJFM} calculated by using sequential Mann-Kendall (SMK) test, where significant change points of the NAO_{DJFM} trend identified are shown as red-dashed vertical lines and the confidence limits (*i.e.* +/-1.96) are shown as blue dashed horizontal lines. No significant change of trend is detected for aa_{DJFM}.

Fig. 3: Same as Fig. 2 but for annual mean sunspot number (Rz_{ann}) (a; b); the 5-yr running mean correlation between annual mean *aa* and Rz_{ann} (corr(*aa*, Rz)) (c; d); December to March mean sunspot area in the Sun's northern hemisphere ($NSSA_{DJFM}$) (e; f); and December to March mean sunspot number asymmetry ($A_{S\,DJFM}$) (g; h). The years when the change points in the trends of Rz_{ann}, corr(*aa*, Rz), $NSSA_{DJFM}$ and $A_{S\,DJFM}$ are shown as the black-dashed vertical lines. For comparison, the years in which the changing points in the NAO_{DJFM} trend are shown as red-dashed vertical lines.

Fig. 4: Same as Fig. 1(a) but for the sub-periods of 1869-1902 (a), 1903-1962 (b), 1963-1995 (c) and 1996-2009 (d). See table 2 for detailed statistical estimates.

878 **Fig. 5:** (a): time series of December to March mean sunspot number (Rz_{DJFM}) with the odd
879 and even numbered SCs shown as red and black circles and the corresponding SC number at
880 the top. The GAM models built by using data for both odd and even numbered SCs (b), only
881 using data from odd numbered SCs (c); and only using data from even numbered SCs (d).
882 See first two rows in of table 3 for detailed statistical estimates.

883 **Fig. 6:** (a): time series of Rz_{DJFM} from all the even numbered SCs with data in the ascending
884 phase showing as red and declining phase as black circles and the corresponding even-
885 numbered SC numbers at the top of the panel. The GAM models built by using data both
886 from ascending and declining phases of even-numbered SCs (b); only using data from the
887 ascending phase (c); and only using data from the declining phase (d). See last four rows of
888 table 3 for detailed statistical estimates.

889 **Fig. 7.** Bootstrap assessment of the winter *aa*-NAO relationship. The black lines represent the
890 10,000 GAMs built by sampling with replacement of the *aa* and the NAO from the declining
891 phase of even-numbered SCs. The mean fit of the 10,000 GAM bootstrapping models are
892 marked as the red curve.

893 **Fig. 8**. The density function of the daily mean *aa* index for the entire period of 1868-2009
894 (black solid), and the four sub-periods of 1868-1902 (red dashed), 1903-1962 (green dotted),
895 1963-1995 (blue dash-dotted), and 1995-2009 (orange long-dashed). Note that only the PDFs
896 of the daily *aa* index for the entire period (1868-2009) and sub-period 1903-1962 (green
897 dotted) are not significantly different at the 0.05 level (p-value = 0.19) based on a
898 Kolmogorov-Smirnoff test [*Press et al.*, 1992]. The other PDFs are tested to be significantly
899 different at the 0.001 level (p-value < 0.001). Moreover, according to the Wilcoxon-Mann-
900 Whitney rank sum test [*Iman*, 1994], the mean values are also significantly different at the
901 0.001 level (p-value < 0.001) for all periods except that between the entire period 1868-2009
902 and the sub-period 1903-1962.

903 **Fig. 9:** (a): same as Fig. 6(d) except that the data from the declining phases of even numbered
904 SCs within the sub-periods of 1869-1902 (red circles), 1903-1962 (green circles), 1963-1995
905 (blue circles) and 1996-2009 (orange circles) are highlighted. Note that only one year
906 (*i.e.*1996) is in the declining phase of even numbered SCs within the last sub-period of 1996-
907 2009. Anomalous years (*i.e*. 1969, 1995 and 1996) were also labeled. Linear fitting of the *aa*-
908 NAO relationship for the sub-periods of1869-1902, 1903-1962 and 1963-1995 are shown in
909 (b), (c) and (d), where the number of samples, estimated R^2 and *p*-value are given on the top
910 of each panel. Anomalous years (*i.e*. 1969 and 1995) were also labeled in (d).
911
912

913 **Table 1.** Estimated coefficients by fitting linear and GAM models to the relationship
914 between aa_{DJFM} and NAO_{DJFM} for the entire period of 1869-2009. Standard errors for the
915 intercept and slope of linear and the intercept for GAM models are in brackets and
916 significant coefficients at the 0.05, 0.01, and 0.001 levels are marked by, "*", "**", and "***".
917 The associated Akaike information criterion (AIC) and effective degree of freedom (EDF) for
918 nonparametric smooth terms are listed for comparison.

919

Period	***Linear Model***				***GAM***			
	intercept	Slope	R^2	AIC	intercept	EDF of *f(aa)*	R^2	AIC
1869-2009	0.36	0.005	0.00	424	0.47***	2.50*	0.08	417
	(0.29)	(0.014)			(0.09)			

920

921

922 **Table 2.** Same as table 1 but for the four sub-periods identified by the SMK test.

923

Period	***Linear Model***				***GAM***			
	intercept	Slope	R^2	AIC	intercept	EDF of *f(aa)*	R^2	AIC
1869-1902	0.27	0.005	0.00	106	0.34	1	0.00	106
	(0.58)	(0.036)			(0.19)			
1903-1962	1.70***	-0.06**	0.13	168	0.60***	1.78**	0.17	166
	(0.40)	(0.02)			(0.12)			
1963-1995	-2.68***	0.13***	0.42	92	0.43**	1.94***	0.50	89
	(0.68)	(0.03)			(0.23)			
1996-2009	0.33	0.01	0.00	48	0.28	1	0.00	48
	(1.30)	(0.06)			(0.31)			

924

925

926

927

928 **Table 3**. Same as table 1 but linear and GAM models were built based the data from even
929 (odd)-numbered SCs, the declining (ascending) phases of odd-numbered SCs, and the
930 declining (ascending) phases of even-numbered SCs.

931

Solar cycle	***Linear Model***				***GAM***			
	intercept	Slope	R^2	AIC	intercept	EDF of *f(aa)*	R^2	AIC
odd NO. SC	0.56 (0.40)	-0.01 (0.02)	0.00	225	0.33** (0.11)	1	0.00	225
even No. SC	0.27 (0.41)	0.02 (0.02)	0.01	206	0.64*** (0.13)	2.39*	0.17	196
ascending odd No. SC	1.06 (0.79)	-0.04 (0.04)	0.04	96	0.24 (0.19)	1	0.04	96
declining odd No. SC	0.43 (0.46)	-0.001 (0.02)	0.00	132	0.40* (0.15)	1	0.00	132
ascending even No. SC	0.97 (0.71)	-0.02 (0.04)	0.01	77	0.63* (0.22)	4.59	0.40	74
declining even No. SC	-0.17 (0.54)	0.04 (0.02)	0.06	133	0.64*** (0.14)	2.43**	0.34	121

932

933

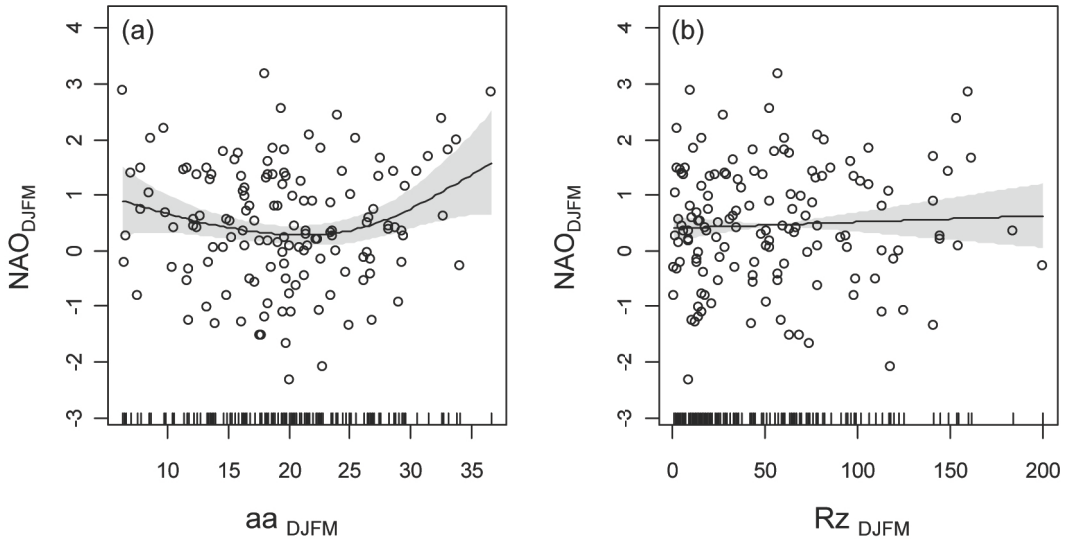
(a)
(b)
NAO DJFM
aa DJFM
Rz DJFM
-3
-2
-1
0
1
2
3
4
10
15
20
25
30
35
0
50
100
150
200

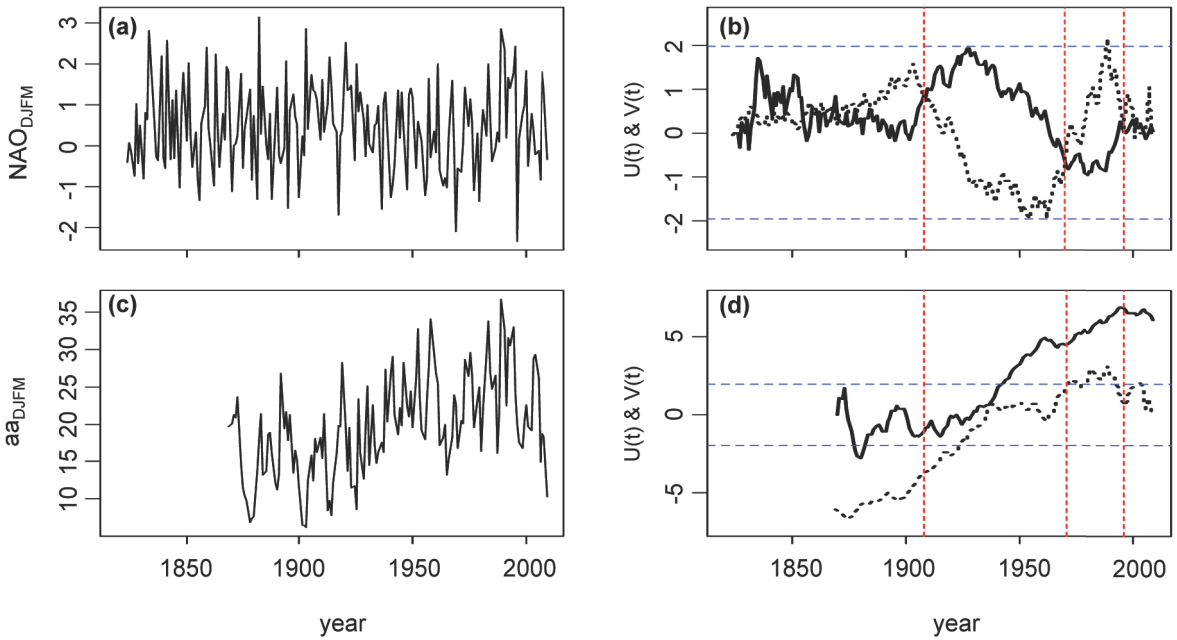
(a)
NAO$_{DJFM}$
(b)
U(t) & V(t)
(c)
aa$_{DJFM}$
(d)
U(t) & V(t)
1850
1900
1950
2000
year
year

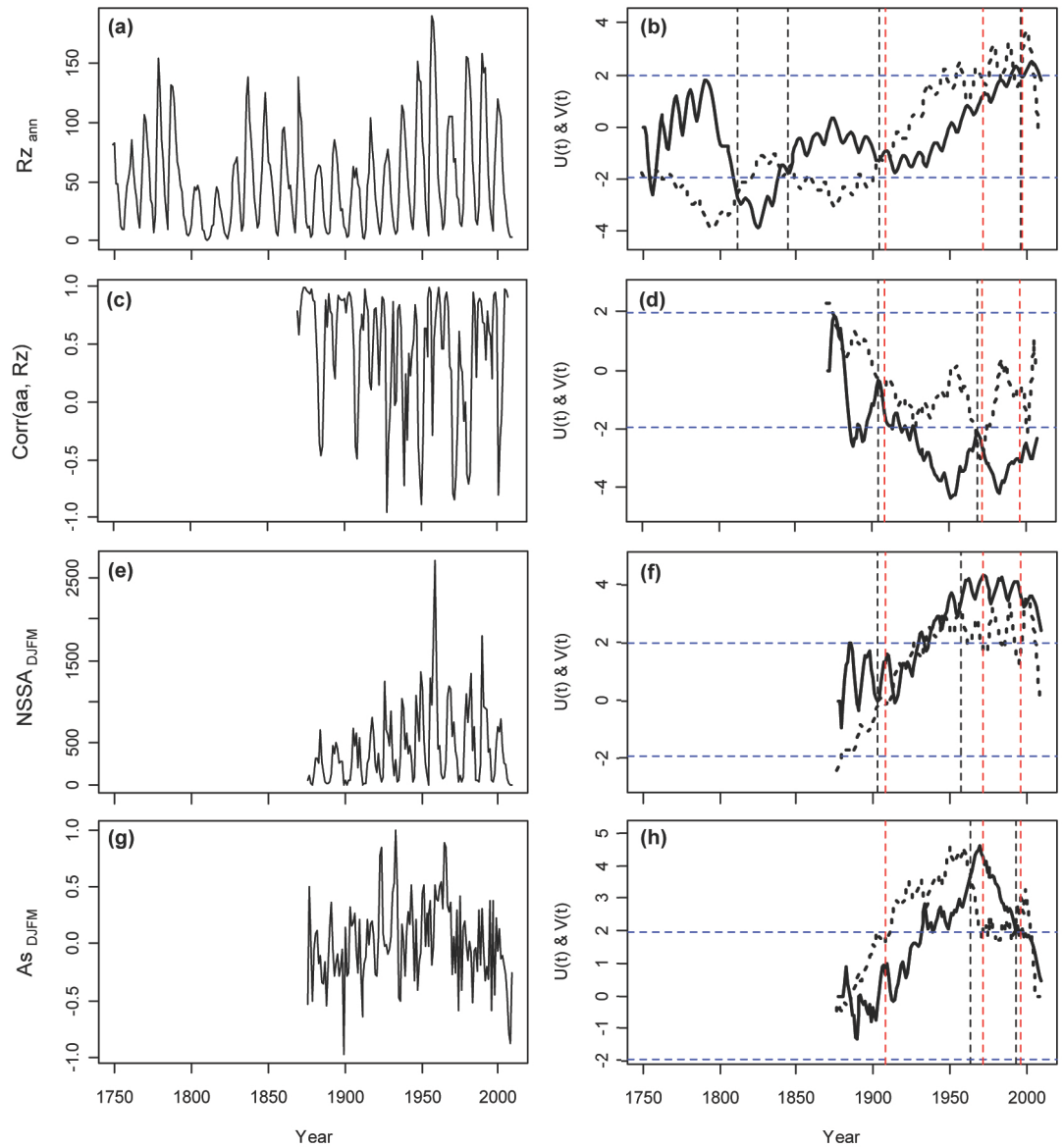
(a)
(b)
(c)
(d)
(e)
(f)
(g)
(h)
Rz ann
Corr(aa, Rz)
NSSA DJFM
As DJFM
U(t) & V(t)
Year
1750
1800
1850
1900
1950
2000

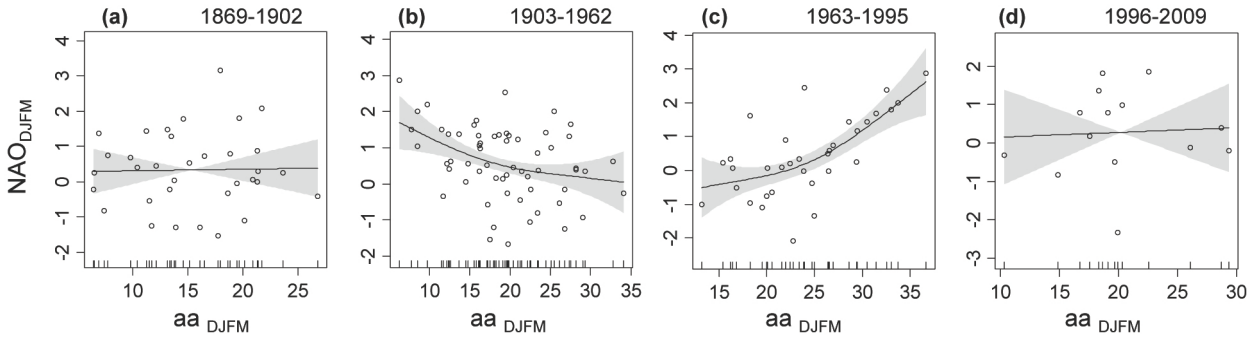
(a) 1869-1902
(b) 1903-1962
(c) 1963-1995
(d) 1996-2009
NAO DJFM
aa DJFM
aa DJFM
aa DJFM
aa DJFM

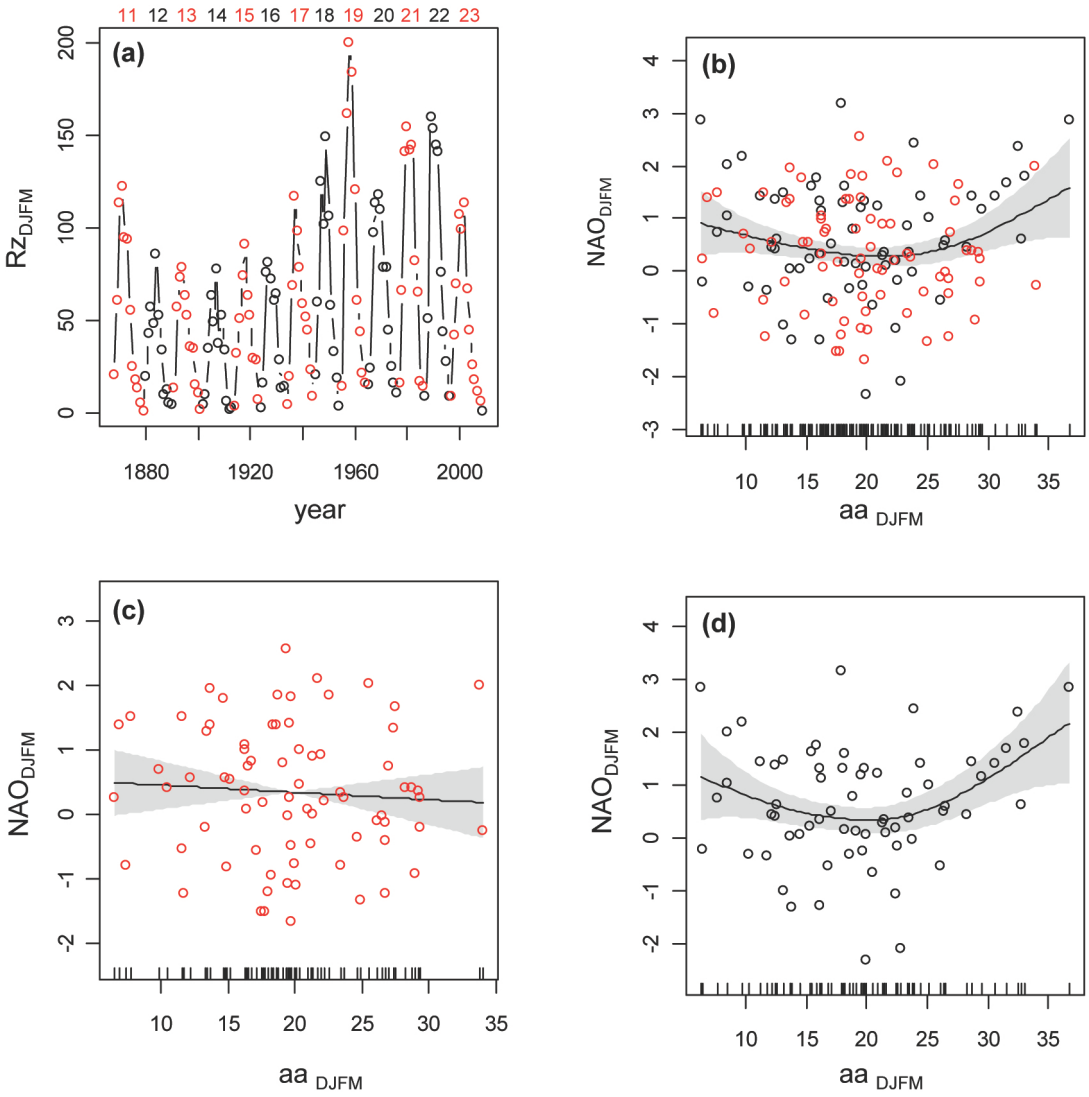
11 12 13 14 15 16 17 18 19 20 21 22 23
(a)
Rz DJFM
year
(b)
NAO DJFM
aa DJFM
(c)
NAO DJFM
aa DJFM
(d)
NAO DJFM
aa DJFM

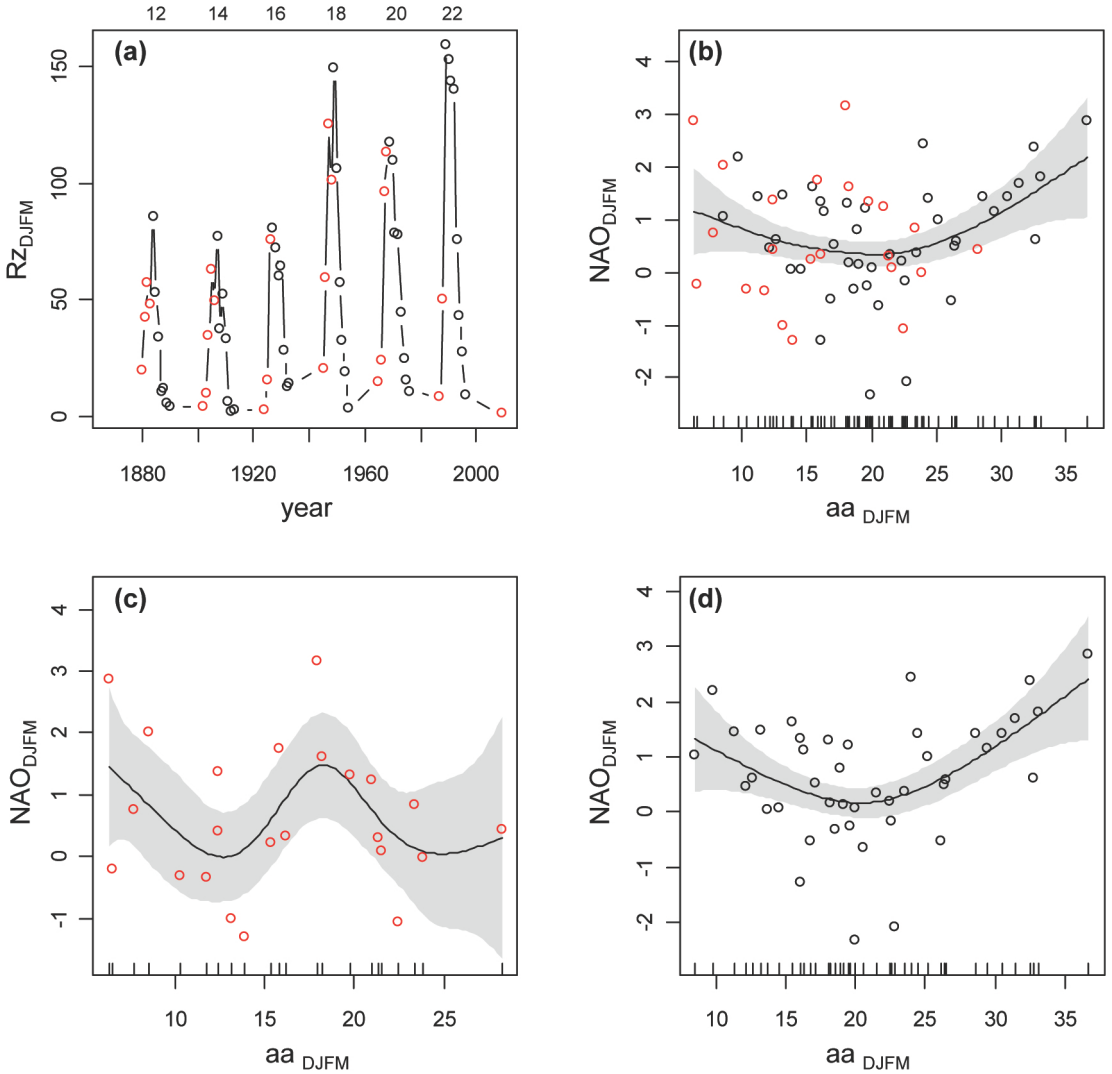
(a)
12
14
16
18
20
22
150
100
50
0
Rz_{DJFM}
1880
1920
1960
2000
year
(b)
4
3
2
1
0
-1
-2
NAO_{DJFM}
10
15
20
25
30
35
aa_{DJFM}
(c)
4
3
2
1
0
-1
NAO_{DJFM}
10
15
20
25
aa_{DJFM}
(d)
4
3
2
1
0
-1
-2
NAO_{DJFM}
10
15
20
25
30
35
aa_{DJFM}

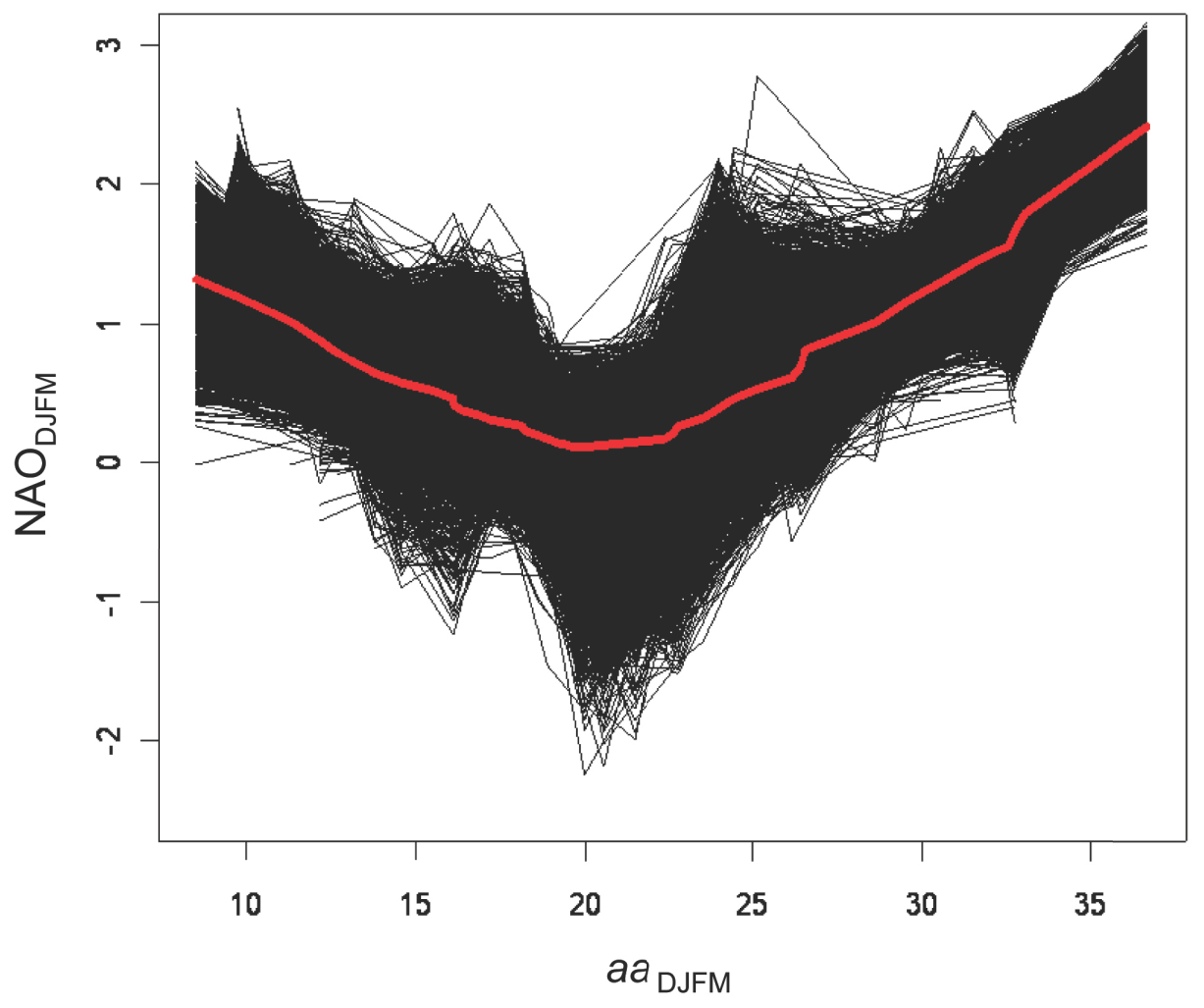
NAO DJFM
3
2
1
0
-1
-2
10
15
20
25
30
35
aa DJFM

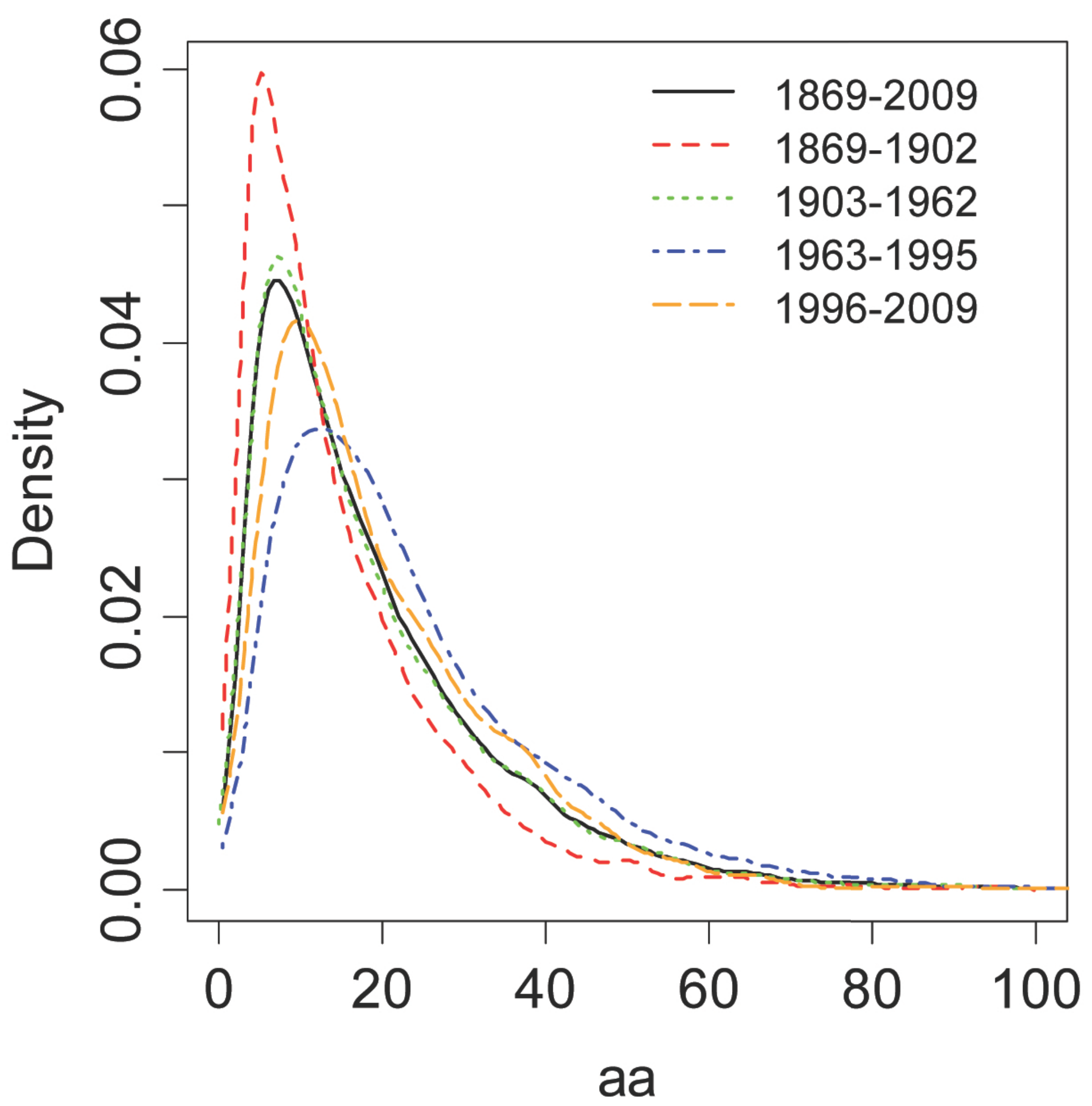
1869-2009
1869-1902
1903-1962
1963-1995
1996-2009
Density
0.00
0.02
0.04
0.06
0
20
40
60
80
100
aa

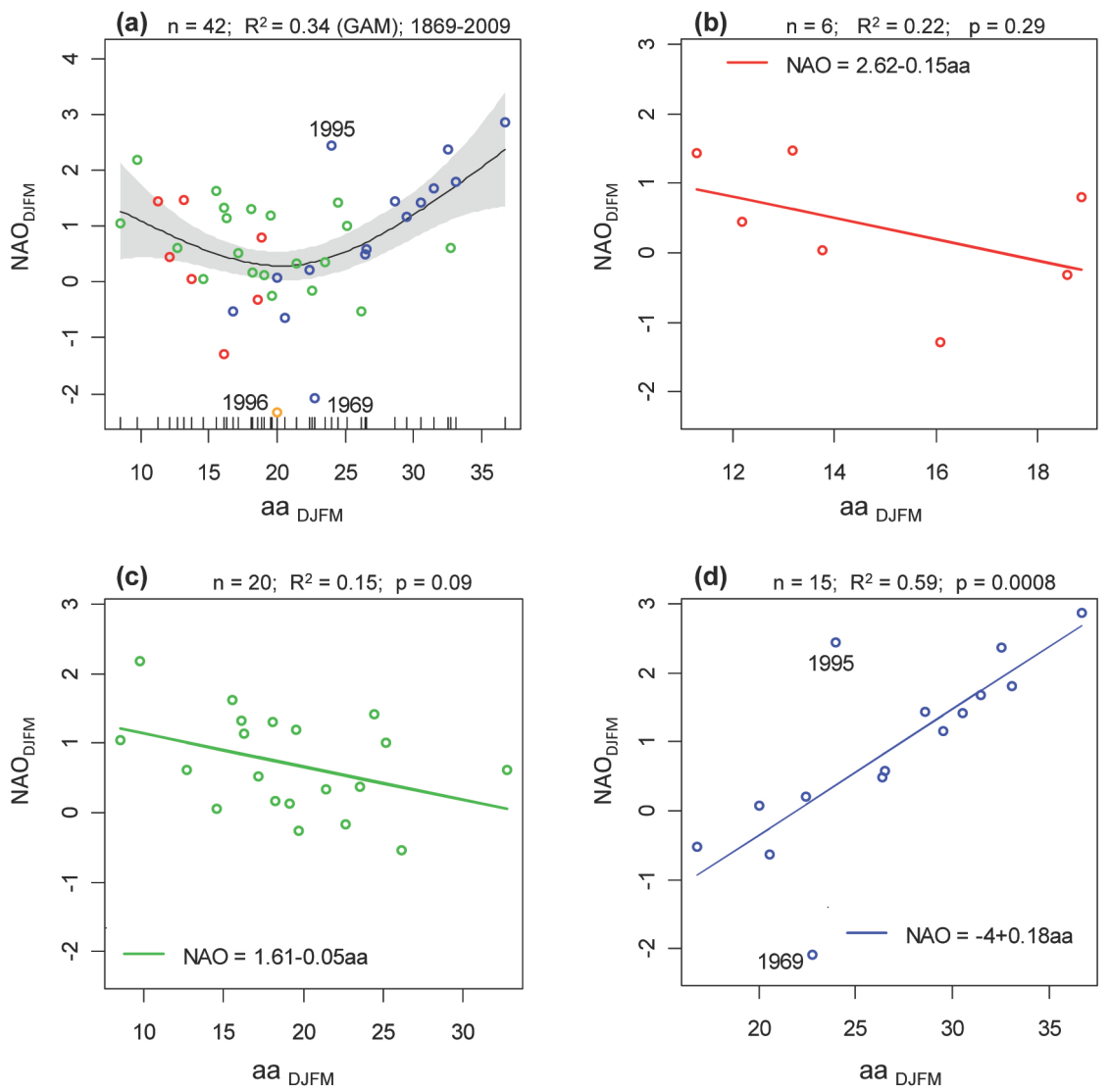
(a)
n = 42; R² = 0.34 (GAM); 1869-2009
1995
1996
1969
NAO DJFM
aa DJFM
(b)
n = 6; R² = 0.22; p = 0.29
NAO = 2.62-0.15aa
NAO DJFM
aa DJFM
(c)
n = 20; R² = 0.15; p = 0.09
NAO = 1.61-0.05aa
NAO DJFM
aa DJFM
(d)
n = 15; R² = 0.59; p = 0.0008
1995
1969
NAO = -4+0.18aa
NAO DJFM
aa DJFM